Spring 2019

Kinetics of HIV-1 Uncoating in C20 Microglial Cells

Melanie Anne Taylor
Missouri State University, mel906@live.missouristate.edu

KINETICS OF HIV-1 UNCOATING IN C20 MICROGLIAL CELLS

A Master's Thesis

Presented to

The Graduate College of

Missouri State University

In Partial Fulfillment

Of the Requirements for the Degree

Master of Science, Cell and Molecular Biology

By

Melanie Anne Taylor

May 2019

KINETICS OF HIV-1 UNCOATING IN C20 MICROGLIAL CELLS

Biomedical Sciences

Missouri State University, May 2019

Master of Science

Melanie Anne Taylor

ABSTRACT

Uncoating is a poorly understood yet required step of HIV-1 replication that is defined as the disassembly of the viral capsid structure. The goal of this project is to characterize uncoating in C20 microglial cells. These cells are a natural target of HIV-1 that are infected to establish latent viral reservoirs and HIV-associated neurological disorders. A stable C20 cell line that expresses TRIM-CypA was established to study the kinetics of uncoating with the CsA washout assay. The expression of TRIM-CypA was confirmed by western blot and the functionality of the protein was confirmed by a viral infectivity assay. Using this cell line, uncoating was found to have an average half-life of 63.3 min. Viral fusion assays determined the kinetics of viral fusion in C20 cells compared to uncoating. The average half-life of viral fusion was found to be 40.9 min. To characterize the effect of CsA on HIV infectivity in C20 cells a viral infectivity assay was performed in the presence and absence of CsA. It was discovered that HIV infectivity was slightly lower in the presence of CsA. The study of uncoating kinetics in microglial cells will give more insight on how HIV establishes infection in brain cells which contributes to a larger goal of developing better therapies, a vaccine, and ultimately, a cure to HIV.

KEYWORDS: HIV-1, viral replication, uncoating, TRIM-CypA, microglia

KINETICS OF HIV-1 UNCOATING IN C20 MICROGLIAL CELLS

By

Melanie Anne Taylor

A Master's Thesis
Submitted to the Graduate College
Of Missouri State University
In Partial Fulfillment of the Requirements
For the Degree of Master of Science, Cell and Molecular Biology

May 2019

Approved:

Amy Hulme, Ph.D., Thesis Committee Chair

Amanda Brodeur, Ph.D., Committee Member

Richard Garrad, Ph.D., Committee Member

Julie Masterson, Ph.D., Dean of the Graduate College

ACKNOWLEDGEMENTS

I would first like to express my sincere gratitude to my committee chair Dr. Amy Hulme for her continuous support, enthusiasm, and patience throughout my thesis writing process. I would also like to thank my committee members Dr. Amanda Brodeur and Dr. Richard Garrad for their support and advisement. I am extremely thankful to my fellow graduate student Zachary Ingram for answering questions that arose in the laboratory during my research process. Lastly, a special thanks to Kate Okland for her assistance during my experimental procedures.

TABLE OF CONTENTS

LIST OF TABLES

LIST OF FIGURES

INTRODUCTION

Disease Relevance

Human Immunodeficiency Virus (HIV) is the virus that can progress to the deadly disease known as Acquired Immunodeficiency Syndrome (AIDS). This virus infects cells of the immune system that express a CD4 receptor (CD4+ cells) which are responsible for identifying and coordinating an immune response to invading pathogens. Cells that express a CD4 receptor include T helper cells, monocytes, macrophages, and dendritic cells. Chemokine co-receptors such as C-C motif chemokine receptor 5 (CCR5) or C-X-C motif chemokine receptor 4 (CXCR4) are common secondary receptors that HIV utilizes for infection in addition to the primary CD4 receptor. As HIV infection progresses, more immune cells are destroyed and the immune system is increasingly damaged, making the body more susceptible to common infections and cancer. The progression from HIV to AIDS takes 8 to 10 years and is marked by extremely low T cell counts and an immune system that is unable to respond to infections.

The HIV/AIDS pandemic is a global health concern. HIV is the world's leading infectious disease killer with approximately 36 million people currently living with HIV/AIDS, many of which are unaware they are infected (UNAIDS, 2018). Individuals unaware of their infection status unknowingly contribute to the spread of the virus. Transmission of HIV follows three major routes: unprotected sexual contact, exposure to contaminated blood or bodily fluids, and perinatal transmission. The virus cannot be transmitted by air or water, saliva, sweat or tears, pets or insects, or sharing toilets, food and drinks (Centers for Disease Control and Prevention [CDC], 2019a). The virus does not survive on surfaces and cannot reproduce on its own. The primary methods of transmission of HIV in the United States is sexual contact and sharing

syringes (CDC, 2019a). Various methods of prevention exist to decrease transmission of the virus.

Antiretroviral therapy (ART) is a combination of drugs used to treat individuals who have been infected with HIV. These drugs target steps of the viral replication cycle to destroy viral infection. The recommended initial regimen for a patient recently diagnosed with HIV-1 is 1 integrase strand transfer inhibitor (INSTI) and 2 nucleoside reverse transcriptase inhibitors (NRTI; (National Institute of Health, 2019)). This combination targets integration and reverse transcription of the virus. Strict adherence to drug regimen is the only way for therapy to be effective. If even one dose is missed, the virus quickly replicates and exponentially increases viral load. ART offers a way to treat side effects of HIV and keep viral load low but cannot cure an infected individual.

Biomedical approaches such as pre-exposure prophylaxis (PrEP) and post-exposure prophylaxis (PEP) have been designed to utilize ART to stop the spread of HIV. PrEP is a medicine taken daily that, when regimen is adhered to, reduces the risk of getting HIV from sex by more than 90% and reduces the risk of those who inject drugs of contracting the virus by more than 70% (CDC, 2019b). This drug therapy is recommended for those who have an HIV positive partner or inject drugs and share needles. PEP is a drug therapy used to treat individuals who have been potentially exposed to HIV to prevent exposure from becoming an infection. PEP medication must be taken once or twice daily for 28 days and must be started within 72 hours of exposure (CDC, 2019c). These medications aim to keep transmission of HIV to a minimum for a healthier society.

No vaccine or cure for HIV/AIDS exists, underscoring the need for additional research of the virus. Current research of HIV replication is conducted in cell lines that HIV infects *in vivo*,

as well as does not infect *in vivo*. In the human body, microglial cells are infected by HIV and are involved in HIV-associated neurological disorders (HAND). Thus, microglial cells should be used in further studies researching HIV infection. Expansion of the current knowledge of HIV replication can lead to new drug targets, therapies, and a vaccine.

HIV Replication Cycle

Early replication. The HIV-1 replication cycle is a nine-step process that can be divided into two parts: early and late replication. The early steps of HIV-1 replication establish infection of the host cell. Binding of the viral envelope to specific receptors on the cell surface initiates infection. The viral envelope is made up of a two-part glycoprotein complex, with gp120 being the surface glycoprotein and gp41 being the transmembrane glycoprotein (Freed, 2001). Gp120 first binds the CD4 receptor on a host cell through a high affinity interaction of the N-terminal extracellular domain of CD4 and a site located between the third and fourth conserved domain of gp120 (Freed, 2001). Once gp120 binds CD4, it undergoes a conformational change that increases the affinity for co-receptors CCR5 or CXCR4 and binds the co-receptor, creating a ternary complex between gp120, CD4, and a co-receptor (Freed, 2001). A conformational change occurs in gp41 that triggers the second step of HIV-1 replication known as membrane fusion. The ectodomain of gp41 is composed of a hydrophobic N-terminus called the fusion peptide, and 2 heptad repeat motifs called the N-helix and C-helix. When the ternary complex between gp120, CD4, and a co-receptor form, a rearrangement occurs in the N-helix and C-helix of gp41, resulting in fusion peptide insertion into the target membrane (Freed, 2001). In this step, gp41 acts to fuse the plasma membrane of the host cell and the lipid bilayer of the viral envelope, consequently releasing the viral capsid into the cytoplasm. The viral capsid is an outer protein

shell structure of the virus that surrounds viral RNA and viral proteins necessary for infection (Freed, 2001).

Once in the cytoplasm, the capsid structure disassembles in a process called uncoating. At this step, the viral complex is called the reverse transcription complex (RTC) and includes several viral proteins such as matrix (MA), nucleocapsid (NC), reverse transcriptase (RT), integrase (IN), and viral protein R (Vpr). The viral RNA is reverse transcribed into double stranded DNA (dsDNA) while remaining associated with the RTC. Once reverse transcription is complete, the complex is referred to as the pre-integration complex (PIC). The PIC is trafficked to the nucleus with help from viral and cellular factors such as microtubules and motor proteins. At the nucleus, the complex containing the viral genome migrates through the nuclear pore complex. This is a capsid-dependent process called nuclear import, that is facilitated by host factors including cleavage and polyadenylation factor 6 (CPSF6), Transportin-3 (TNPO3), and NPC (Nuclear pore complex) proteins. Once inside the nucleus, integration occurs in which integrase inserts the viral dsDNA genome into the host cell chromosome. Integration completes the early steps of HIV replication which are depicted in Figure 1. At this stage, the viral DNA is called the provirus and acts a gene in the host cell (Freed, 2001).

Late replication. The late steps of HIV-1 infection begin with transcription of the provirus to produce viral RNA molecules that are translated into functional proteins. The three polyproteins synthesized are Gag, Env, and Pol. Gag and Env polyproteins provide structure while Pol polypeptide provides enzymatic functions to the virus. Once the provirus is transcribed and translated, the newly produced viral proteins work together to form a virion.

Following translation, the virus undergoes the steps of trafficking, assembly, budding, and maturation to form a functioning virion. The MA protein targets and binds to the plasma

membrane of the host cell, while NC proteins and CA proteins interact to encapsidate viral RNA, packaging the viral genome within the virion (Freed, 2001). MA also functions to recruit and localize Env proteins to the cell surface assembly sites through direct and indirect interactions (Checkley, Luttge, & Freed, 2011). The virus then pinches off from the host cell membrane to create an immature virion that is surrounded by a layer of cell membrane in a process called budding. Maturation of the virion is marked by proteolytic cleavage of polyproteins. The Gag protein is proteolyzed into MA, CA, NC, and p6 while the Env protein is broken down into surface or gp120 (SU) and transmembrane or gp41 (TM) proteins. The Pol polyprotein is broken down into protease (PR), RT, and IN (Frankel & Young, 1998). Tat, Rev, Vpu, Vif, Vpr, and Nef are the six accessory proteins that have various functions. Figure 2 depicts all the viral polyproteins and accessory proteins, and their locations in the virion. The resulting mature virion has a membrane decorated with envelope proteins on the outside, matrix proteins on the inside, and holds a conical capsid made of CA proteins that stores the remaining viral proteins and two copies of viral RNA, as depicted in Figure 2. The resultant virion is capable of binding to a new host cell to resume the viral replication cycle.

Uncoating

Capsid structure. Uncoating is the disassembly of the viral capsid and is a required step of early HIV-1 infection that is not fully understood. The viral capsid is a conical structure composed of 1,000 to 1,500 CA protein monomers (Briggs et al., 2004). Capsid monomers have two domains, an N-terminal domain and a C-terminal domain. The CA protein is composed of predominantly alpha helices, with the C-terminal domain housing 4 alpha helices and the N-terminal domain housing 6 alpha helices (Berthet-Colominas et al., 1999). CA monomers

polymerize to form many hexameric and some pentameric structures that constitute the viral capsid. The N-terminal domains typically form a rigid, 6-fold ring on the inside of the polymer while the C-terminal domains form a mobile outer belt that is capable of rotation in compliance with the inner N-terminal ring (Pornillos, Ganser-Pornillos, & Yeager, 2011). These hexameric polymers form a lattice that contains few pentameric structures that allow the structure to have curved edges. Although the typical shape of the capsid is conical, the capsid possesses morphological abilities and at times takes on a spherical or tubular shape (Li et al., 2016). The capsid encloses essential viral components for infection. Two copies of the viral RNA genome, NC, RT, IN, and viral accessory proteins are all found inside the capsid core (Accola, Öhagen, & Göttlinger, 2000). The capsid structure is an important component of viral uncoating.

Models of uncoating. The exact process by which the viral capsid uncoats has not been established. Three uncoating models exist to propose the method by which uncoating occurs, but it is possible that HIV-1 uncoats using different methods or a combination of methods when infecting different types of cells. The first suggested method of uncoating is rapid core disassembly in which once the virus enters the host cell, the capsid immediately falls apart. As reverse transcription takes place between viral entry and integration, RTCs were examined for viral proteins to attempt to determine the point at which the virus uncoats. The complexes were found to have high densities of MA, RT, and IN proteins and low densities of CA proteins (Fassati & Goff, 2001). From these data, it was concluded that the capsid core must rapidly dissociate following viral entry before the formation of the RTC. Since these studies, this first model has been largely discounted because CA protein has been detected in the cytoplasm associated with the RTC and the discovery of cellular factors, such as microtubules, that interact with the capsid (McDonald et al., 2002; Peng et al., 2014).

The second model of uncoating suggests that the capsid core remains intact immediately following viral entry, and gradually disassembles in the cytoplasm during reverse transcription and transport of the RTC to the nucleus. This cytoplasmic uncoating model proposes that uncoating is promoted by several factors, including CA contact with cellular factors in the cytoplasm and molecular rearrangements that accompany reverse transcription. Evidence of this relationship between uncoating and reverse transcription was found when treatment with reverse transcription inhibitors delayed uncoating (Hulme, Perez, & Hope, 2011). Further studies have suggested that uncoating occurs after the first strand transfer of reverse transcription (Cosnefroy, Murray, & Bishop, 2016). These discoveries show that the steps of uncoating and reverse transcription may have some influence on each other, and since reverse transcription is a cytoplasmic event, the cytoplasmic model is plausible.

The nuclear pore complex model of uncoating suggests that the capsid remains intact until encountering the nuclear pore complex, where the intact capsid is too large to travel through the nuclear pore. Uncoating is thought to occur while the capsid is tethered at the nuclear pore complex and after the completion of reverse transcription. The mutation of CA protein, Q63/67A, was found to produce virial complexes that improperly uncoat and are defective in nuclear import and integration (Dismuke & Aiken, 2006). This link between capsid uncoating and nuclear import supports the nuclear pore complex model. Nuclear import proteins such as TNPO3 and NPC proteins have been found to influence the rate of uncoating, providing further evidence that uncoating occurs at the nuclear pores (Lee et al., 2010).

Viral and cellular factors. Uncoating is a complicated process that requires interactions from other steps of the viral replication cycle in order to occur. Previous studies have investigated the importance of CA structure in relation to the kinetics of uncoating of the viral

capsid. Mutant A92E was found to significantly increase the rate of uncoating while mutants E45A and N74D delayed the rate of uncoating (Hulme, Kelley, Okocha, & Hope, 2015). Mutant A92E has a mutation in CypA binding loop in CA, and successfully infects cells when CypA is inhibited (Qui, Yang, & Aiken, 2008). This mutant explores the relationship between CypA and CA, and how that relationship affects viral infectivity. Mutant E45A has a mutation in Helix 2 of CA (Yamashita, Perez, Hope, & Emerman, 2007). This mutant does not have the same dependence on TNPO3 and NPC proteins that wildtype HIV does (Lee et al., 2010). Mutant N74D uses a different pathway for nuclear import, utilizing NUP155 instead of NUP153 (Lee et al., 2010). This type of mutation allows investigation of cellular factors required for nuclear import of HIV-1. All of these capsid mutants alter the kinetics of uncoating and consequently decrease overall viral infectivity (Forshey, von Schwedler, Sundquist, & Aiken, 2002; Hulme et al., 2015; von Schwelder, Stray, Garrus, & Sunquist, 2003).

The uncoating of the capsid core is a complex step of viral infection that may require the involvement of other steps of viral infection, including reverse transcription and integration. As previously discussed in the cytoplasmic uncoating model, there is a relationship between reverse transcription and uncoating. Additionally, some models suggest that as reverse transcription progresses and flexible RNA is converted into more rigid double stranded DNA, the capsid core must remodel to accommodate this change (Campbell & Hope, 2015). Integrase is the viral protein that integrates the viral genome into host DNA. This viral enzyme was found to interact with the viral core. A study introduced mutations to IN and observed a decrease in viral capsid core yield and stability (Briones, Dobard, & Chow, 2010). Thus, it is possible that IN helps stabilize the capsid core. Furthermore, mutations in IN resulted in virions depleted of the cellular protein Cyclophilin A (CypA) that produced unstable viral capsid cores (Briones et al., 2010).

These discoveries suggest that integrase and CypA interaction may have an effect on capsid core stability.

CypA is an important cellular molecule when discussing uncoating as it binds to CA to potentially affect uncoating. CypA binds directly to the N terminal domain of the capsid core (CA_{NTD}) via a Gly89-Pro90 peptide bond, and functions to catalyze the cis/trans isomerization of the peptide bond (Bosco, Eisenmesser, Pochapsky, Sundquist, & Kern, 2002). The isomerization results in a conformational change of the CA_{NTD} but the effect that CypA binding to CA has on uncoating varies. Recent experiments investigating this have found conflicting results, concluding that CypA destabilizes the HIV-1 capsid core, CypA stabilizes the core to inhibit HIV-1 uncoating, and, in some cell types, CypA does not affect HIV infectivity (Fricke, Brandariz-Nuñez, Wang, Smith, & Diaz-Griffero, 2013; Hatziioannou, Perez-Caballero, Cowan, & Bieniasz, 2005; Shah et al., 2013). Regardless, it is noted that CypA is an important variable in HIV-1 uncoating and further research on this cellular factor is needed.

The breakdown of the nuclear envelope is not necessary for HIV-1 to establish infection in cells, meaning that HIV-1 can infect non-diving cells. Virus enters the nucleus by capsid proteins interacting with various cellular proteins including CPSF6, TNPO3, and NPC proteins. CPSF6 is a cellular protein that shuttles between the nucleus and cytoplasm, and colocalizes with the RTC in the cytoplasm to aid in nuclear import (Peng et al., 2014). CPSF6 interacts with HIV-1 CA protein in the binding pocket formed between neighboring CA_{NTD} and CA_{CTD} (Bhattacharya et al., 2014). This protein contains a Serine/Arginine rich nuclear localization signal (NLS) on its C terminus that, when removed in mutant $CPSF6_{1-358}$, inhibits HIV-1 infection by a defect in nuclear entry (Lee et al., 2010; Peng et al., 2014). This protein plays a large role in nuclear entry of HIV-1 by interaction with CA protein but is not the only key player.

TNPO3 is a protein that transports cargo into the nucleus and influences the nuclear localization of CPSF6 (Kataoka, Bachorik, & Dreyfuss, 1999). Because infectivity of HIV-1 is inhibited by knockdown of TNPO3, it is thought that TNPO3 is involved in nuclear import (Lee et al., 2010). This influence on nuclear import may be indirect by interaction with CPSF6, or straightforward by TNPO3 directly binding to the HIV-1 CA (Zhou et al., 2011).

NPC proteins are also of interest when discussing nuclear import. Two NPC proteins in particular, NUP358 and NUP153, were found to be cellular factors required for HIV-1 infection (Brass et al., 2008). NUP358, also referred to as RanBP2, is a protein that protrudes from the NPC into the cytoplasm of the cell and is involved in various nucleo-cytosplasmic transport pathways (Zhang, Mehla, & Chauhan, 2010). This NPC protein has a CypA homology domain that interacts with viral capsid protein (Schaller et al., 2011). Although this interaction has been discovered, the exact mechanism in which these proteins interact is still under investigation. NUP153 is a part of the NPC that has filaments extended into the nucleoplasm, instead of the cytoplasm (Strambio-De-Castilla, Niepel, & Rout, 2010). CA also interacts with NUP153 to aid in nuclear import (Price et al., 2012). These findings suggest that CA interaction with NPC proteins is necessary for nuclear import of the RTC, and due to this interaction, NPC proteins may play a role in uncoating.

Other cellular factors involved in uncoating are microtubules and motor proteins. Disruption of microtubules, dynein, dynein heavy chain 1 (DYNC1HC1), and KIF5B delays uncoating (Lukic, Dharan, Fricke, Diaz-Griffero, & Campbell, 2014). KIF5B of the Kinesin-1 family may be involved in both uncoating and nuclear import. An interaction dependent on both KIF5B and the viral capsid results in NUP358 relocation from the NPC to the cytoplasm (Dharan et al., 2016). This interaction may directly or indirectly influence uncoating and nuclear import.

Microtubule associated proteins have also been found to have influence on steps of HIV-1 infection. The dynein adapter protein Bicaudal D2 (BICD2) binds the viral capsid and mediates trafficking of the viral complex, and depletion of this protein inhibits uncoating (Dharan et al., 2017). It is also thought that HIV-1 exploits the functions of diaphanous-related formins (DRFs), which manage actin nucleation and microtubule stabilization, to coordinate uncoating and control microtubule stabilization for virus transport (Delaney, Malikov, Chai, Zhao, & Naghavi, 2017). It is probable that other microtubule associated proteins (MAPs) that function in the same way as DRFs are also involved in capsid interaction for viral complex trafficking and uncoating.

There are two models that propose the mechanism of interaction between microtubules and motor proteins with the capsid. The tug of war model suggests that kinesin and dynein pull the capsid apart concurrently (Gaudin, de Alencar, Arhel, & Benaroch, 2013). The NPC- and kinesin-mediated uncoating model suggests that dynein chaperones the capsid core to the nuclear pore complex, where interaction between the capsid and NPC directly induces uncoating (Campbell & Hope, 2015) or interaction at the NPC anchors the capsid while kinesin provides the force necessary for uncoating (Campbell & Hope, 2015). The exact method of interaction between HIV-1 capsid and microtubules and motor proteins is still under debate, but it can be agreed upon that they are essential factors in the viral replication process.

To determine how cellular factors affect uncoating, the kinetics of uncoating were compared in OMK cells and HeLa cells. The uncoating of wildtype virus occurred faster in HeLa cells than in OMK cells while the N74D mutant had a longer delay of uncoating in HeLa cells, possibly due to a factor that is present in more abundance in one cell line than another

(Hulme et al., 2015). Because that factor(s) remains unknown, the effect of differences in cellular environments on uncoating is an area of interest that is worth further researching.

Microglial Cells

As the resident macrophage of the brain, microglial cells are important for maintaining the health of the central nervous system. Microglial cells serve an immune surveillance function while at rest by continuously sampling their environment with highly motile protrusions and sensing changes through surface receptors, such as receptors for complement fragments, immunoglobulins, adhesion molecules, and inflammatory stimuli (Nimmerjahn, Kirchhoff, & Helmchen, 2005). When signs of infection or injury are discovered, the microglial cells rapidly convert to an active state and release molecules to begin an immune response. These molecules are pro-inflammatory mediators and include cytokines, chemokines, reactive oxygen species (ROS), and nitric oxide (Saijo & Glass, 2011). The release of these molecules promotes inflammation and is intended to isolate the infectious agent to prevent further contact with body tissues. However, when pro-inflammatory molecules are released excessively by microglial cells pathological forms of inflammation may result and contribute to neurodegenerative disease (Saijo & Glass, 2011). Therefore, microglial cells play a large role in protecting the CNS from infection but can also be detrimental when they are inappropriately activated.

HIV infection of microglial cells are linked to HIV-associated neurological disorders (HAND) found in HIV/AIDS patients. HAND is an area of interest due to its negative effects on brain function. Three subcategories of HAND exist to categorize the degree of neurological impairment caused by HIV infection. Asymptomatic neurocognitive impairment (ANI) is classified by abnormality in two or more cognitive abilities with no functional impairment, while

mild neurocognitive disorder (MND) is cognitive impairment with mild functional impairment (Elbirt et al., 2015). The most serious of the three subcategories is HIV-associated dementia (HAD). HAD is classified as marked cognitive impairment with marked functional impairment (Elbirt et al., 2015). The mechanism by which HIV infections causes HAND is still unknown.

HIV infects cells that express CD4 receptors such as T-cells, macrophages, and dendritic cells, as well as microglial cells. HIV cannot cross the blood brain barrier, so it does not directly infect the brain but enters the brain by infecting migrating monocytes and lymphocytes that cross the blood brain barrier (BBB) (Elbirt et al., 2015). Once inside the brain, infected monocytes transform into macrophages and microglial cells. The infection is spread throughout the brain by cells from the macrophage lineage. Macrophages and microglial cells express neurotoxic molecules that activate astrocytes, leading to increased BBB permeability (Elbirt et al., 2015). Infected monocytes and lymphocytes migrate across the BBB easier with increased permeability and continue to spread the infection. Although microglial cells are not primarily infected by HIV in the CNS, once infected cells migrate into the CNS and differentiate into several types of macrophages, microglial cells become infected and play a role in spreading the infection throughout the brain.

Two models exist that hypothesize how HIV positive cells cause neurodegeneration. The first model is a direct model that states HIV infected monocyte-derived cells release viral proteins gp120, Tat, and Vpr that interact directly with neurons causing neuronal death (Elbirt et al., 2015). The direct model suggests that microglial cells, along with other monocyte-derived cells, interact firsthand with neurons. The indirect model hypothesizes that neuronal death is caused by the inflammatory response against HIV infection and HIV proteins released by directly infected cells (Elbirt et al., 2015). While the direct model blames physical contact

between viral proteins and neurons for neuronal death, the indirect model blames the overwhelming inflammatory response to HIV infection. While the exact method of neuronal death leading to HAND is unknown, the importance of studying the details of HIV infection in microglial cells remains. The study of uncoating in microglial cells will uncover more in-depth information about early infection in the central nervous system that eventually leads to HAND.

Highly active antiretroviral therapy (HAART) is the current therapy method used to treat patients with HIV and, when the treatment is strictly adhered to, is effective at keeping the infection minimal and below levels of detection. One reason it is thought that HAART is unable to completely eliminate the virus from an infected individual is the difficulty to reach latently infected cells in viral reservoirs. A viral reservoir is a cell or an anatomical site in association with which a replication-competent form of the virus accumulates, meaning it is able to replenish the population of infected cells and is not defective, and persists with more stable kinetic properties than in the main pool of actively replicating virus (Blankson, Persaud, & Siliciano, 2002). Viral reservoirs ensure that the virus is able to maintain infection throughout the body by providing an escape from immune response efforts. There are two different types of latency that occurs in reservoirs. “Pre-integrated latency” occurs when the pre-integration complex (PIC) exists in the cytoplasm of an infected cell (Lambotte, Deiva, & Tardieu, 2006). Cells with pre-integrated latency could be active or inactive, and eventually the pre-integration complex will migrate from the cytoplasm into the nucleus to integrate itself into the cellular DNA and produce virions to spread the infection. The second type of latency is “post-integrated latency” in which the linear viral DNA complex, or PIC, is integrated into the cellular DNA of inactive cells, and when the cell becomes active later on, the integrated viral form is transcribed, and viral RNA is produced allowing the production of new virions (Lambottee et al., 2006). Reservoir cells are

latently infected by HIV and contribute to the persistence of infection despite the efforts of drug treatment. The major reservoir cells in CNS are microglia, perivascular macrophages, and astrocytes (Garcia-Mesa et al., 2017). It is important to study the early steps of HIV infection in microglial cells because they are a subtype of latent cells located in the viral reservoir in the brain.

Immortalized primary microglial cells isolated from human brain tissue are ideal to use while studying HIV infection in microglial cells. The use of this cell line, called C20, ensures that data collected closely resembles what actually happens when HIV infects the human brain. Many previous HIV investigations are conducted using cells that are not naturally infected by HIV. This can be problematic as cell to cell protein variability may impact the pathology of HIV infection, making the data potentially misleading. C20 cells are immortalized cells that originate from human cortical brain tissue obtained from adults undergoing brain surgery at University Hospitals of Cleveland (Garcia-Mesa et al., 2017). Primary microglial cells are delicate and difficult to maintain in culture, so the cells were immortalized to allow experimentation. To immortalize, the primary microglial cells were infected with vesicular stomatitis virus G enveloped simian virus 40 (VSVG SV40) expressing large T antigen and selected in the presence of 2 ug/mL of puromycin. The cells were then superinfected with VSVG hTERT-neomycin viral particles to express human telomerase reverse transcriptase and antibiotic-resistant colonies were selected in the presence of 2 ug/ml puromycin and 600 ug/ml neomycin (Garcia-Mesa et al., 2017). Once the cells were immortalized, characterization took place. It was confirmed that the C20 cells were of human origin using PCR amplification of the human CYCT1 gene from DNA isolated from the immortalized human microglial cells (Garcia-Mesa et al., 2017). Confirmation of the species of origin is an important step in ensuring that the cells will provide the most

accurate data. Upon characterization, it was found that the C20 cells express key microglial surface markers, have microglial-like morphology, demonstrate appropriate migratory and phagocytic activity, and have the capacity to mount an inflammatory response characteristic of primary microglia (Garcia-Mesa et al., 2017). These characteristics, especially cell signaling, demonstrate how the C20 cell line is a close representation of real microglial cells and, therefore, is an ideal cell line to use to investigate HIV infection in the CNS.

TRIM-CypA and CsA Washout Assay

TRIM5α and TRIM-CypA are a part of the TRIM5 family of proteins that act as restriction factors to retroviruses. TRIM5 proteins exist in nature in different isoforms. TRIM5α is composed of RING, B-box, coiled-coil, and SPRY domains (Li et al., 2016). A related TRIM protein named TRIM5-Cyclophilin A (TRIM-CypA) is expressed in owl monkeys by a retrotransposition of Cyclophilin A (CypA) into TRIM5 intron 7 (Nisole, Lynch, Stoye, & Yap, 2004). The CypA domain exits on the TRIM-CypA protein where the SPRY domain exists on the TRIM5α (Li et al., 2016). Aside from the difference in one prominent domain, TRIM5α and TRIM-CypA are similar proteins. Their sizes are comparable with TRIM5α being 55 to 60 kDa and TRIM-CypA being 45 kDa (Nepveu-Traversy, Bérubé, & Berthoux, 2009). TRIM5 proteins have the ability to bind to the capsid of incoming retroviruses, such as HIV, to restrict infection. In the TRIM-CypA form of the TRIM5 protein, the CypA domain acts to bind to viral capsid proteins. This interaction occurs via flexible loops on the CypA domain and allows TRIM-CypA to form a hexagonal net on the viral capsid to act as a restriction factor (Li et al., 2016). The restrictive properties of TRIM-CypA are utilized in research to better understand characteristics of the HIV capsid.

Cyclosporin A (CsA) is a drug that binds to TRIM-CypA and inhibits its function. Thus, in the presence of CsA, uncoating of the HIV capsid can occur and the virus establishes infection (Figure 3). The CsA washout assay is an infection assays done in the presence of CsA with cells that contain TRIM-CypA and are used to study the rate of uncoating. In these assays, CsA is washed out at different timepoints and the amount of uncoating of that virus can be determined at specific timepoints by measuring infectivity. To be resistant to TRIM restriction, a virus would have to have already uncoated at the time when CsA is washed out. Flow cytometry is used to determine infectivity by percentage of GFP positive cells. Cells that express GFP have completed the step of uncoating, therefore providing a method to determine the amount of uncoating at a specific timepoint. A control washout is done using ethanol in place of CsA.

Previous uncoating studies done in OMK and HeLa cells have utilized the CsA washout assay. OMK cells naturally express TRIM-CypA while HeLa cells in this experiment were engineered to express TRIM-CypA. Parallel CsA washout assays found that HIV-GFP uncoated significantly faster in HeLa cells than in OMK cells (Hulme et al., 2015). Variability of cellular proteins in OMK and HeLa cells is thought to be the explanation of the difference in uncoating kinetics between the two cell lines because HIV uses cellular factors to establish infection.

There are multiple assays in the field used to study uncoating. The *in situ* uncoating assay uses dual labeled virus with GFP-Vpr to detect virions and S15-mCherry labeled viral membrane that is lost upon viral fusion (Campbell, Perez, Melar, & Hope, 2007). At various points of infection, cells are fixed and stained for CA protein to determine whether uncoating has occurred (Campbell et al., 2007). The fate of capsid assay is another method used to study uncoating. This assay fixes cells at various timepoints postinfection, uses ultracentrifugation, and cell extracts are

examined for the separation of soluble capsid protein from capsid cores (Yang, Luban, & Diaz-Griffero, 2014).

The CsA washout assay was used in this study because of its many benefits. The CsA washout assay is beneficial because it removes any virus that uncoats that is not replication competent from the data because the read out is GFP positive infected cells. *In situ* uncoating assays and fate of capsid assays do not remove replication incompetent virus because they test for capsid protein to determine if uncoating has occurred and are not selective for capsid in virus that is replication competent. The usage of TRIM-CypA in this assay is beneficial because the protein binds directly to the capsid and restricts uncoating directly. The entire CsA uncoating assay is done in live cells, allowing infectivity to run its course before cells are fixed while *in situ* uncoating assays and fate of capsid assays fix cells at various timepoints post-infection. Often the fate of capsid assay work is done past when uncoating occurs. The *in vivo* aspect of this assay provides data that is similar to what happens in the human body which is useful in developing a vaccine or cure.

Hypothesis and Aims

The goal of this project is to characterize the kinetics of HIV-1 uncoating in C20 microglial cells. This research question is relevant because neither OMK cells nor HeLa cells are among the types of cells infected by HIV-1 in the human body, while C20 cells are. Cellular proteins differ in each cell line which is relevant to HIV-1 infection because the virus utilizes cellular factors to establish infection. Research conducted in non-naturally infected cells may confer results that differ from naturally infected cells. Thus, it is essential to study the kinetics of early infection in cells such as microglial cells that are infected by HIV-1 in the human body. I

hypothesize that C20 microglial cells will have a faster rate of uncoating when infected with HIV-GFP in comparison to OMK cells and HeLa cells, with uncoating kinetics being more similar to HeLa cells because they are a human cell line. To test this hypothesis, three aims were proposed. The first aim was to characterize the effect of CsA on HIV-1 infectivity in C20 cells and the timing of viral fusion. The second aim was to establish a C20 cells that stably expresses TRIM-CypA. The third aim was to determine uncoating kinetics of wild type HIV-1 in the established C20-TRIM-CypA cell line.

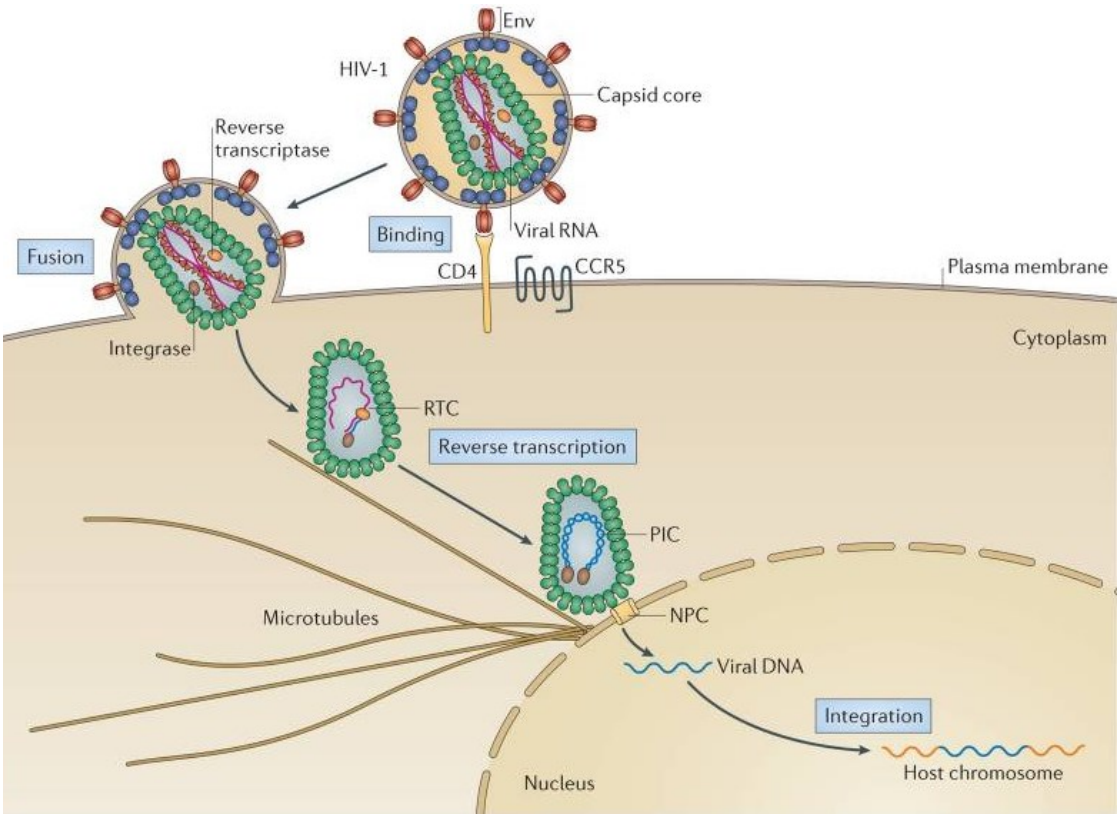

Figure 1. Early steps of the HIV-1 replication cycle. This image was obtained from "HIV-1 capsid: the multifaceted key player in HIV-1 infection" (Campbell & Hope, 2015).

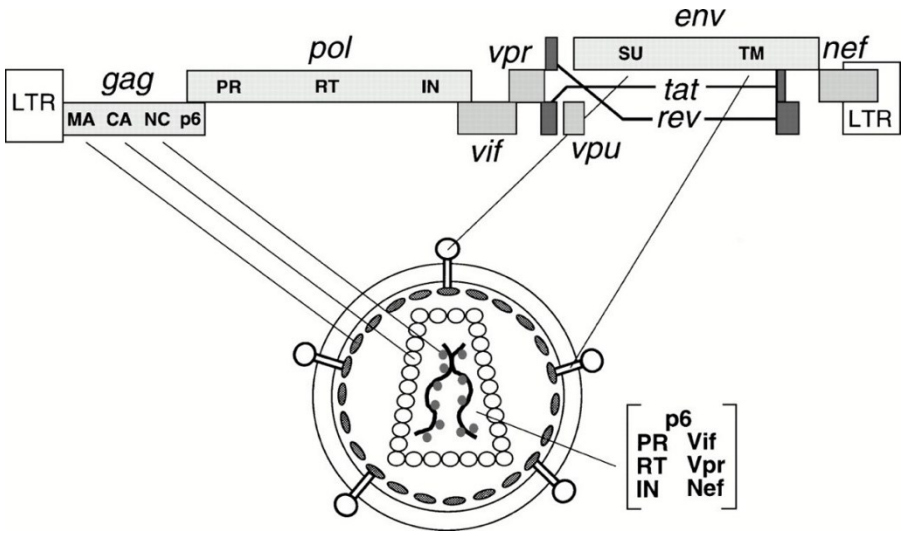

Figure 2. HIV-1 polyproteins and accessory proteins in the viral genome. This image was obtained from “HIV-1: fifteen proteins and an RNA” (Frankel & Young, 1998).

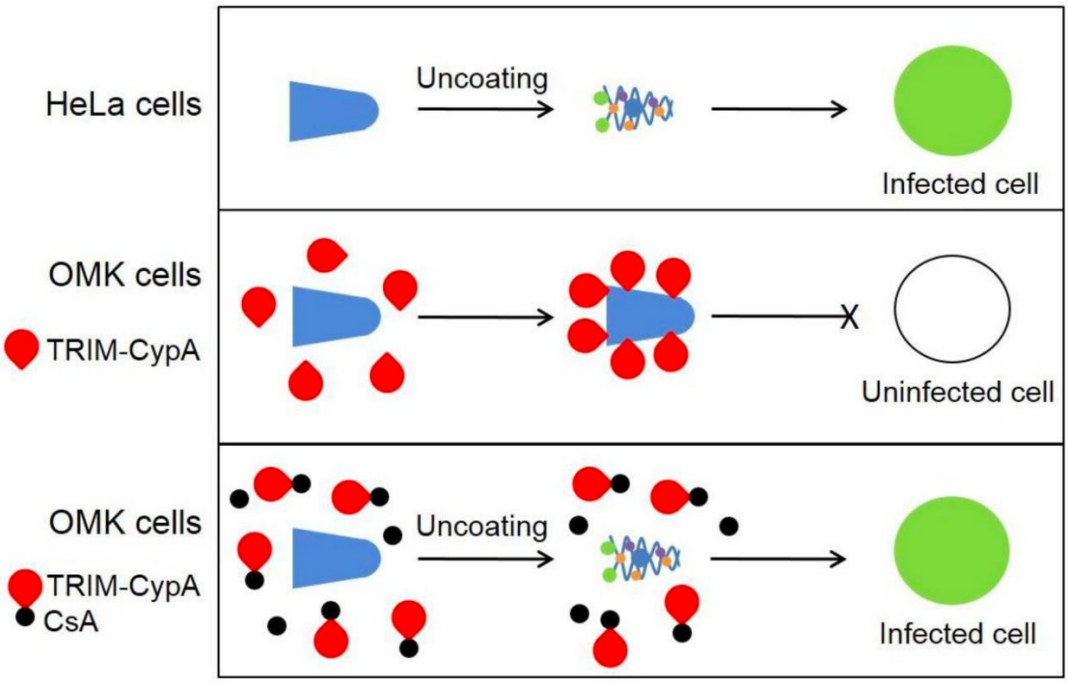

Figure 3. The interactions behind the CsA washout assay. Interaction of CsA with TRIM-CypA inhibits the protein and diminishes the restriction of HIV-1 infection. This image was obtained from “The CsA washout assay to detect HIV-1 uncoating in infected cells” (Hulme & Hope, 2014).

MATERIALS AND METHODS

Maintain and Culture Cell Lines

The use of cells in this project did not require Institutional Review Board approval. The 293T cell line utilized to make HIV-GFP is a human embryonic kidney cell line obtained from American Type Culture Collection. The CHME3 cell line is a human microglial cell line and the TCN14 cell line is CHME3 cells engineered to express TRIM-CypA, and both cell lines were obtained from the Naghavi Lab at Northwestern University (Janabi, Peudenier, Héron, Ng, & Tardieu, 1995). The C20 cell line is a human microglial cell line obtained from Karn Lab at Case Western Reserve University (Garcia-Mesa et al., 2017). All cultured cell lines used were adherent cells that were grown in plastic 10 cm tissue culture dishes. Cells were grown in an incubator set at 37°C with the presence of 5% CO2. All experiments involving cells were done in a tissue culture hood with the use of sterile technique. The media used for 293T cells was Dulbecco's Modified Eagle Media (DMEM; Corning) with the addition of 10% fetal bovine serum (FBS; Atlanta Biological), 100 U/ml penicillin streptomycin (Corning), and 292 µg/ml L-gutamine (PSG; Corning). C20 and C2-9 microglial cells used DMEM media with 5% FBS, 100 U/ml penicillin streptomycin, 292 µg/ml PSG, and 1% Sodium Pyruvate (Corning). Media used for C2-9 cells also contained 100 µg/ml of hygromycin B (Corning).

Cells adhered to the bottom of the plate and when they grew to confluency, they had to be split in order to continue actively growing. The 293T cells and the C20 cells and C2-9 cells were split using different methods. To split 293T cells, media and trypsin (Corning) were warmed in a 37°C water bath before media was aspirated from the tissue culture plate and 1 ml of trypsin was carefully added to the plate. After washing the cells in trypsin, the trypsin was aspirated from the plate and the plate was placed in the 37°C incubator for approximately 2 minutes. Following

incubation, 10 ml of media was added to the plate to inactivate the trypsin. The cells were resuspended and 1 ml of the cell suspension was transferred to a new 10 cm plate containing 10 ml of fresh media. The plate was gently rocked and then placed in the 37°C incubator. Cells were observed under a microscope daily and split every 2 to 3 days.

To split the C20 and C2-9 microglial cell lines, the media and trypsin was warmed in a 37°C water bath, the media was aspirated from the 10 cm plate containing the cells, and 5 ml 1X phosphate-buffered saline (PBS; Corning) was added to the plate to wash away any residual media. The PBS was aspirated and 3 ml of trypsin was added before the plate was put into the 37°C incubator for 2 to 3 minutes. Following incubation, 7 ml of media was added to the plate to inactivate the trypsin and resuspend the cells. A new 10 cm plate was prepared with 10 ml of fresh media and 2 ml of the cell suspension was transferred to the new plate and stored in the 37°C incubator. The cells were observed daily and split every 3 to 4 days.

At times when cells were to be left unattended for long periods of time or to retain a stock, it was necessary to freeze cell lines. To freeze cells, a freeze media was first made. This consists of 4 ml C20 media, 500 dimethyl sulfoxide (DMSO; Sigma Aldrich), and 500 µl of FBS. The cells were split into a 15 ml conical tube and spun at 1,000 x g at 4°C for 3 minutes. The media was removed without disturbing the pellet and the pellet was resuspended in 2 ml freeze media and 1 ml of the solution was aliquoted into two cryovials. The vials were placed in a Nalgene Cryo Freezing Container and stored at -80°C.

Cells were thawed from the frozen stock stored at -80°C. To thaw cells that were frozen down from a 6 well plate, a new 6 well plate was prepared by adding 3 ml of warm media to each well. The cryovial containing the frozen cells was held in a warm water beaker until it thawed. The 1ml of cells in the vial was slowly transferred to the 6 well plate. The plate was

incubated for 3 hours, then the media was removed and replaced with 4 ml of fresh media. Two days later, media with antibiotic was added. To thaw cells that were frozen down from a 10 cm plate, the cryovial containing the cells was held in a warm water beak until it thawed. The 1 ml of cells in the tube was transferred to a 15 ml tube and 10 ml of media was slowly added to the tube. Next, 11 ml from the tube was slowly transferred to a 10 cm plate and then 5ml of fresh media was added. The plate was incubated for 3 hours and then the media was removed and replaced with 15 ml of fresh media.

HIV-GFP Virus Production

HIV-GFP is a single round virus made from two plasmids, the viral genome plasmid with a mutated envelope gene and GFP, and a vesicular stomatitis virus (VSV-G) envelope plasmid. The genome plasmid is a source of viral RNA and viral proteins, with the exception of envelope protein. The envelope plasmid encodes for the VSV-G envelope protein, which allows the virus to enter any kind of cell via endocytosis. The use of 2 plasmids create a single round vector, enabling the virus to only infect a cell once and preventing it from making more virus in that cell due to the mutated envelope protein. This makes HIV-GFP a replication defective virus.

A polyethylenimine (PEI) transfection of 293T cells was used to make HIV-GFP virus. To begin, 293T cells were seeded into a 10 cm plate so that they would be 80-90% confluent on the day of transfection. A transfection mixture was made containing 1 ml DMEM, 6 µg HIV-GFP proviral plasmid, 4 µg CMV-VSV-g plasmid, and 40 µl PEI (Polysciences). The mixture was incubated at room temperature before being added in a dropwise manner to the media of a 10 cm dish containing 293T cells. The dish was then incubated for 24 hours. The media was aspirated from the 10 cm dish and replaced with 10 ml of fresh, warmed media, and the cells

were then incubated for 16-18 hours. The media containing virus was then transferred from the 10 cm dish to a 15 ml conical tube using a serological pipet. The virus was then filtered using a syringe attached to a 0.45 um filter. The virus was stored at -80°C in 1 ml aliquots in cryovials.

TCSH Virus Production

To engineer a cell line that expresses TRIM-CypA, a virus was made that contains genes for the TRIM-CypA (TC) protein and hygromycin (H) resistance (TCSH). To make TCSH virus, a PEI transfection of 293T cells was done. C20 cells were plated in 8 wells of a 12 well plate to be 80-90% confluent on the day of transfection. A mixture containing 200 µl of DMEM, 4 µg of pLXSN-TRIMCypa (TCSH) plasmid (Mamede, Sitbon, Battini, & Courgnaud, 2014), 4 µg of VSV-g plasmid, and 8 µl of PEI was combined and incubated at room temperature for 15 minutes. To each well, 104 µl of the transfection mixture was added in a dropwise manner. The plate was then incubated for 24 hours. The media was aspirated from the plate and replaced with 1 ml of fresh, warmed media per well, and the cells were then incubated for 16-18 hours. The media containing virus was then transferred from the 12 well plate to a 15 ml conical tube using a serological pipet. The virus was then filtered using a syringe attached to a 0.45 um filter. The virus was stored at -80°C in 1 ml aliquots in cryovials.

Hygromycin Kill Curve

A hygromycin kill curve was established to determine the concentration of hygromycin B needed to kill C20 cells that did not contain the gene for hygromycin resistance. C20 cells were plated in a 6 well plate. A different concentration of hygromycin B in media was added in each well (Table 1). The first run of this experiment used concentrations of 0 µg/ml, 100 µg/ml, 200

µg/ml, 300 µg/ml and 400 µg/ml and the cells were observed for 6 days. To better clarify which concentration of hygromycin would be optimal for selection of cells, the experiment was repeated a second time with lower concentrations including 0 µg/ml, 50 µg/ml, 100 µg/ml, 150 µg/ml, and 200 µg/ml. The cells were observed to determine which concentration killed all cells in a reasonable amount of time.

C2-9 Cell Line Production

Figure 4 is a summary of the process of establishing the C2-9 cell line. The C20 cells infected with different dilutions of TCSH, ½ dilution, ¼ dilution, 1/8 dilution, 1/16 dilution, 1/16 dilution, and no virus as a control, in a 6 well plate. The day after infection, the media was replaced with warm C20 media. Two days after infection, the media was replaced with C20 media containing hygromycin B that was at a concentration determined by the hygromycin kill curve method. In the 6 well plate, one well containing cells infected with a 1/16 dilution of TCSH received media without drug to serve as a control. Antibiotic selection continued until all cells had died in the no virus control well. The cells in the 6 well plate in the ¼ and ½ dilution were maintained until they were confluent and healthy enough to split to a 10cm plate. The C20 cells infected with ½ dilution of TCSH and ¼ dilution of TCSH were split into 10cm plates. Once confluent, cells from each dilution were frozen down while others were kept in culture.

The cells were counted and diluted to 1 cell/600 µl and plated on 96 well plates in attempt to isolate colonies. This method failed to produce viable colonies and a new approach was taken. The C20 cells infected with ¼ dilution of TCSH were thawed and grown in culture. The cells were counted, and a series of dilutions were made to achieve four dilutions of cells on four 10cm plates: 100 cells/plate, 75 cells/plate, 50 cells/plate, and 25 cells/plate. The cells were

allowed to grow for 18 days before 8 colonies were picked from the 100 cells/plate diluted plate and for 21 days before 12 colonies were picked from the 75 cells/plate diluted plate.

To isolate clones, individual colonies had to be lifted off of the plate. Pieces of filter paper were autoclaved and soaked in 1 ml of trypsin in a 6 well plate. Tweezers were used to place individual pieces of filter paper on each colony and lift. The filter paper with the colonies was placed in a 24 well plate with 1ml of C20 media. The cells were allowed to grow in the 24 well plates for 3 days before the filter paper was removed and the media was replaced with C20 media containing hygromycin B.

The cells remained under antibiotic selection as they were grown and spilt as depicted by Figure 5. From the 24 well plate the cells were transferred to a 12 well plate. Once cells were confluent in the 12 well plate, the cells were split to prepare a whole cell lysate for western blot as described in the western blot methods section, and the remainder of cells were plated in a new 12 well plate. Once confluent, the cells were split into a 6 well plate until confluent then frozen and stored at -80°C.

Western Blot

To confirm presence of the TRIM-CypA protein in the new cell lines, a western blot was performed with an antibody targeted to the HA tag on TRIM-CypA. A whole cell lysate was produced from each cell line. Cells were lysed by adding 200 µl of 1X Laemmli Sample Buffer (Bio-Rad) containing β-mercaptoethanol (Fischer Scientific) to a confluent well of cells in a 12 well plate. The cells became viscous as they lysed, and the lysate was transferred to an Eppendorf tube. This cell lysate was then boiled at 100°C for 3 minutes, cooled, and centrifuged for 20 seconds at full speed. The samples were stored at -20°C until ready for use. 10% Tris-HCl

Bio-Rad Ready Gels (Bio-Rad) were assembled in a Bio-Rad gel rid according to the manufacturer's instructions and 12 µl of an all blue standard protein ladder (Bio-Rad) was loaded into the first well. Protein samples were boiled at 100°C for 5 minutes, and then 40 µl of each sample was loaded onto the gel. The gel was run at 200 V for 40 minutes.

Following electrophoresis, the proteins and ladder were transferred from the gel to a membrane using a Bio-Rad Transblot Semi-Dry Electrophoretic Transfer Cell. The membrane was pre-wet in dH_2O for 2 minutes, then soaked in Towbin Transfer buffer for 45 minutes. When the gel finished running, it was removed from the cassette, rinsed in dH_2O, and equilibrated in transfer buffer for 30 minutes. Extra thick filter paper was also soaked in transfer buffer. The transfer sandwich was assembled in the following order- filter paper, gel, membrane, filter paper, and then flipped. The gel was then transferred at 15 V for 35 minutes.

Following transfer, the membrane was rinsed in dH_2O and blocked in 10 ml of 3% low-fat powdered milk in TBS for 1 hour. The membrane was then rinsed with two changes of 1X TBS-T, and then washed with 1X TBS-T for 5 minutes. The blot was exposed to the primary anti-HA rat 3F10 antibody (Roche Diagnostics) a 1:2000x in 3% Fraction V (Fischer Scientific)/TBS-T, overnight at 4°C.

Two brief rinses of TBS-T were performed followed by three washes with TBS-T for 5 minutes each. The anti-rat HA secondary antibody was diluted in 3% low-fat powdered milk/TBS and added to the membrane in a small container. The membrane was incubated for 1 hour. Next, the membrane was washed with two brief rinses of TBS-T and three washes with TBS-T for 5 minutes each. To visualize the membrane, the SuperSignal West Dura Extended Duration Substrate system (ThermoFischer) was used to detect chemiluminescence of horseradish peroxidase (HRP). On a piece of Saran wrap, 500 µl of SuperSignal West Dura

Stable Peroxide Buffer (ThermoFischer) was mixed with 500 µl of SuperSignal West Dura Luminol/ Enhancer Solution (ThermoFischer). The membrane was placed on the enhanced chemiluminescent (ECL) substrates for 5 minutes. Then, the membrane was wrapped in a fresh piece of Saran wrap. In a dark room, the membrane wrapped in Saran wrap was placed on a piece of film for 1 minute and developed. The membrane was placed on a second piece of film for 10 days and then developed.

Test for Infectivity and Virus Titration

This method can also be used as a virus titration to determine the amount of virus to use for certain assays. From an 80-90% confluent plate, cells were split onto a new petri plate as normal and the remaining cell/media mixture was placed into a 15 ml conical vial. A Bright-Line 1475 hemocytometer (Hausser Scientific) was used to determine cell count. Before use, the Hemocytometer was cleaned using a KIM Wipe and ethanol. Under the tissue culture hood, a glass cover slip was placed on top of the hemocytometer and 15 µl of cells were added. The hemocytometer was focused under a microscope and the number of cells in two 4X4 sections was counted separately and recorded. A concentration of 7,500 cells/well was calculated and cells were plated in a 96 well plate. For each virus tested, at least 6 wells of a 96 well plate were used and 3 wells of uninfected cells in cell culture media served as a negative control for flow cytometry. To each well, 100 µl of cells and media was added, using cell culture media to bring the cell mixture to the total volume. The calculated number of cells and media was added to a 15 ml conical tube, and a multichannel micropipette was used to add 100 µl of the cell mixture to each well. The 96 well plate was then labeled with initials, virus name, and date, and placed in the 37°C incubator overnight.

To aid in infecting cells, 1X polybrene (Santa Cruz Biotechnology) media was made in a 15 ml conical tube and 2X polybrene media was made in an Eppendorf tube. All media was aspirated from the 96 well plate, and 100 µl of 1X media was added to every well except H1 and H2 (see Figure 6), which had 100 µl of 2X media added. To H1, 100 µl of HIV-GFP virus was added and, to H2, 100 µl of positive control virus was added. Nothing was added to H3 as it was the negative control. The multichannel micropipette was used to mix the media and virus in H1 and H2 by carefully pipetting up and down 3 times to create a ½ dilution of the original sample of virus. Next, 100 µl was transferred from H1/H2 to G1/G2 and mixed with the media in the wells by pipetting up and down 3 times to make a ¼ dilution. The serial dilution was continued by transferring 100 µl to each subsequent well and mixing each well by pipetting up and down 3 times. The 100 µl from the last set of wells was discarded in bleach solution and the 96 well plate was placed in the 37°C incubator overnight.

Media was aspirated from all of the wells and replaced with 200 µl of fresh media. The plate was then placed in the 37°C incubator overnight. All of the media was aspirated from the 96 well plate and 100 µl of trypsin was added to each well. The plate was incubated at 37°C for 3-5 minutes. The cells were viewed under a microscope to determine if they appeared to be "peeling up", and the 96 well plate was lightly tapped to help loosen cells. The cell/trypsin mixture was resuspended in each well using a multichannel pipette, and 100 µl of 2% paraformaldehyde (Santa Cruz Biotechnology) was added to each well. The plate was wrapped in parafilm and aluminum foil and incubated at 4°C overnight. The fixed samples were then run on a C6 Accuri flow cytometer with detector (laser) FL1 (488), standard filter (533/30 BP), and GFP fluorochrome with run limits of 10,000 events or 80 ul and fluidics set at fast. for GFP to determine the percentage of infected cells.

CsA Washout Assay

To study the kinetics of viral capsid uncoating, CsA washout assays were performed with C2-9 cells. The night before the assay, cells were seeded out in a 96 well tissue culture plate with 7,500 cells per well to yield 70-80% confluence on the day of the washout assay. There are 9 timepoints (0, 15 min, 30 min, 45 min, 1 hr, 2 hr, 3 hr, 4 hr, and 5 hr) and each timepoint is performed in triplicate with CsA and with EtOH. Three wells served as a positive control that were continuously treated with CsA and 3 wells served as a negative control that were continuously treated with EtOH. In addition, 6 wells of uninfected cells were continuously incubated in cell culture media as a negative control for flow cytometry. Therefore, 66 wells were plated with 7,500 cells in each well.

To begin the assay, a spinoculation mastermix of media was made for each experimental condition in a 15 ml conical tube with enough media to add 100 µl to each well. The cell culture media was incubated in a 37°C water bath for 5-10 min to bring the temperature up from 4°C but below or near 16°C in order to synchronize infection. The mastermix contained C20 media, 5 µg/µl polybrene, 2.5 µM CsA or EtOH, and 1/25 dilution of HIV-GFP virus. The media was aspirated from each well, except the negative control with uninfected cells, and 100 µl of spinoculation media was added. The 96 well plate was spinoculated at 1200 x g at 16°C for 1 hour and incubated at 16°C for approximately 1 hour. The media from all of the wells, except the uninfected cells, was aspirated and the washout for the 0 hr timepoint was performed by adding 200 µl warmed cell culture media. The other wells received 100 µl warmed CsA or EtOH media, and the plate was placed in the 37°C incubator until the 15 min timepoint. The washout was performed at the 15-minute timepoint by aspirating the CsA and EtOH media from the appropriate wells and replacing it with 200 µl of warmed C20 media. The washouts for the 30

min, 45 min, 1 hr, 2 hr, 3 hr, 4 hr, and 5 hr timepoints were performed in the same manner, and then the plate was incubated at 37°C for 2 days.

Following the 2-day incubation, the cells were harvested. Media was aspirated from each well, 100 µl of PBS (Corning) was added to each well and aspirated, and then 100 µl of trypsin (Corning) was added to each well. The plate was incubated at 37°C for 5 minutes until the cells detached and the cells were resuspended using a multichannel pipet. Then, 100 µl of 2% paraformaldehyde was added to each well, the plate edges were wrapped in parafilm and the entire plate was wrapped in foil and stored at 4°C.

To determine the percentage of cell successfully infected by HIV-GFP, flow cytometry was performed using a C6 Accuri flow cytometer to provide the percentage of GFP positive cells. Because the experiment was performed in triplicate, with 3 wells for each timepoint, the averages of the 3 wells for each timepoint and control were calculated. For each timepoint, the average percentage of GFP positive cells for the ethanol control was subtracted from the average percentage of GFP positive cells for CsA treatment to normalize the data. The standard deviation and standard error for the average of each timepoint were calculated. To calculate the half-life of uncoating, the two timepoints that half of the maximum percentage of GFP positive cells falls in were graphed, and the trendline equation was utilized. The highest percentage of GFP positive cells were normalized to 100% and the remaining of the data was calculated by dividing the percentage of GFP positive cells by the highest value of GFP positive cells and multiplied by 100. The standard error was normalized in the same fashion, by dividing the original standard error by the highest percentage of GFP positive cells and multiplying by 100.

Viral Fusion Assay

The viral fusion assay was conducted to study the rate at which the virus fused with the cell. The night before the assay, C20 and C20 2-9 cells were seeded out to obtain 7,500 cells/well in a 96 well plate and 70-80% confluence on the day of the assay. Three wells were needed for each timepoint (0 hr, 15 min, 30 min, 45 min, 1 hr, 2 hr, 3 hr, and 4 hr). For a positive control, 3 wells for each cell line were continuously treated with the fusion inhibitor BafilomycinA (BafA) (company) and, as a negative control, 3 wells for each cell line were uninfected and continuously incubated in cell culture media. This resulted in 33 wells plated for each cell line.

To begin the viral fusion assay, the media was aspirated from each well and a spinoculation mastermix media was made. This media contained C20 media, 2.5 µM CsA, 5 µg/µl polybrene, and 1/25 dilution HIV-GFP, and 100 µl was added to each well except the BafA constant and uninfected wells. A separate spinoculation media mix was made that contained 10 nM BafA, in addition to the other components in the spinoculation mastermix, and 100 µl was added to the BafA constant wells. The plate was spinoculated at 1200 x g at 16°C for 1 hour and incubated at 16°C for 1 hour.

Following spinoculation, the media was aspirated from all wells except the uninfected cells. The 0 hr timepoint was performed by adding 200 µl warmed BafA and CsA containing media to the appropriate wells and the BafA constant wells, and warmed C20 media with CsA was added to the remaining wells. The plate was placed in the 37°C incubator until the 15min timepoint when the media was aspirated and 200 µl of BafA and CsA containing media was added to the appropriate wells. This BafA addition was continued in the same manner for the 30 min, 45 min, 1 hr, 2 hr, 3 hr, and 4 hr timepoints. The 96 well plate was incubated at 37°C for 1 day.

Following incubation, the media was aspirated from all wells and 100 µl of warmed C20 media was added to each well. The plate was then incubated at 37°C for 1 day. To harvest the cells, the media was aspirated from each well and replaced with 100 µl of PBS, which was aspirated and replaced with 100 µl of trypsin. The plate was incubated at 37°C until the cells detached from the plate. The cells were then resuspended by pipetting with a multichannel pipette. Next, 100 µl of 2% paraformaldehyde was added to each well to fix the cells. The plate's edges were wrapped in parafilm, the entire plate was wrapped in foil, and the plate was stored at 4°C.

Flow cytometry was run using a C6 Accuri flow cytometer to determine the percentage of cells infected by the virus and thus expressing GFP fluorescence. As this experiment was done in triplicate, the average of 3 wells for each timepoint and control was calculated. The standard deviation and standard error for each average timepoint was calculated. The values for each timepoint were normalized to the 0 hr timepoint being 0% GFP positive cells. To find the viral fusion half-life, the two timepoints that half of the maximum percentage of GFP positive cells falls in were graphed, and the trendline equation was utilized. The value of the highest percentage of GFP positive cells was normalized to 100% and the remaining values followed this trend by dividing by the highest value and multiplying by 100. The standard errors for each timepoint were converted to a new normalized value by dividing by the highest value for percentage of GFP positive cells and multiplying by 100.

Table 1. Hygromycin kill curve in C20 cells. Two hygromycin kill curves were established to determine the optimal amount of hygromycin to use when growing C20-TC cells under hygromycin selection. The concentration of hygromycin in each well of the 6-well plate for each experiment is shown.

Well	Concentration of hygromycin	
	Run 1	Run 2
1	0 μg/ml	0 μg/ml
2	100 μg/ml	50 μg/ml
3	200 μg/ml	100 μg/ml
4	300 μg/ml	150 μg/ml
5	400 μg/ml	200 μg/ml
6	500 μg/ml	

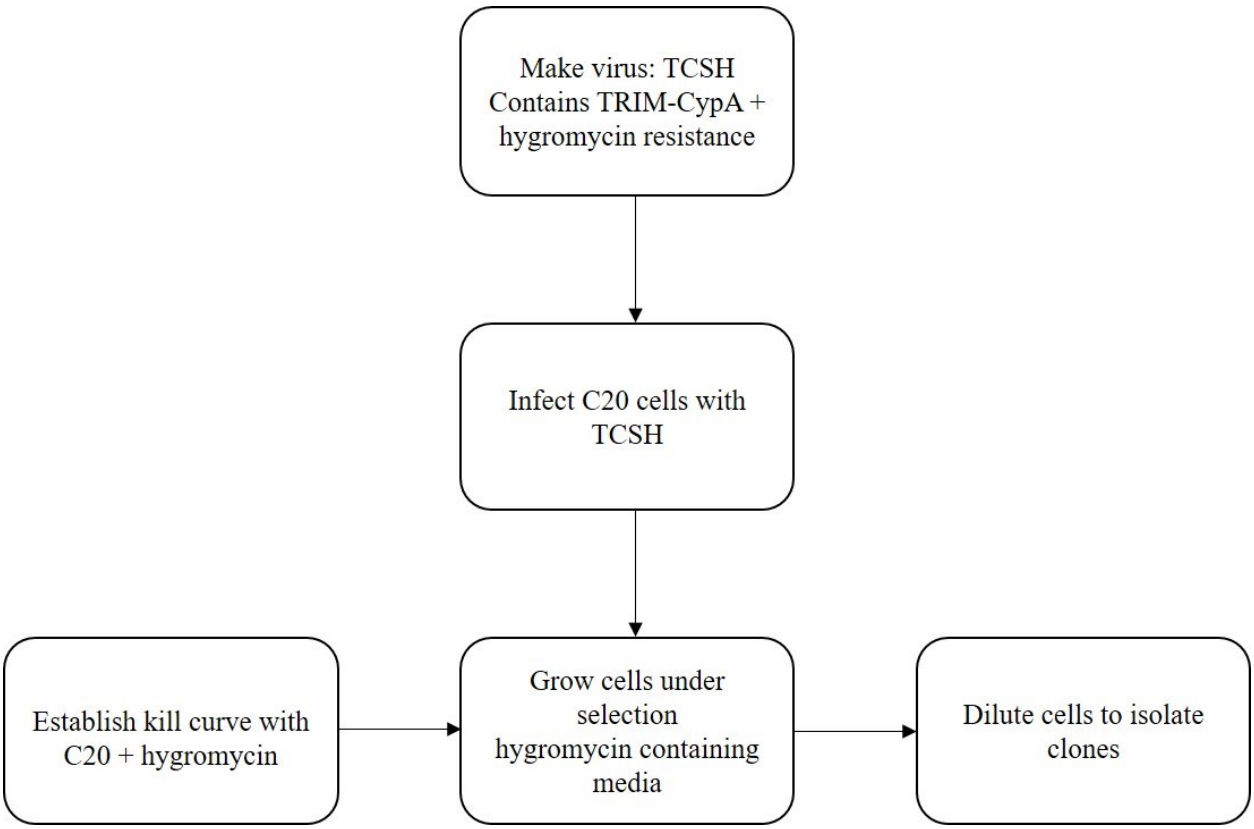

Figure 4. Flow chart simplifying the steps of generating C20-TC cell line. Generation of the C20-TC cell line began with engineering TCSH virus and proceeded through the steps of the flowchart as shown.

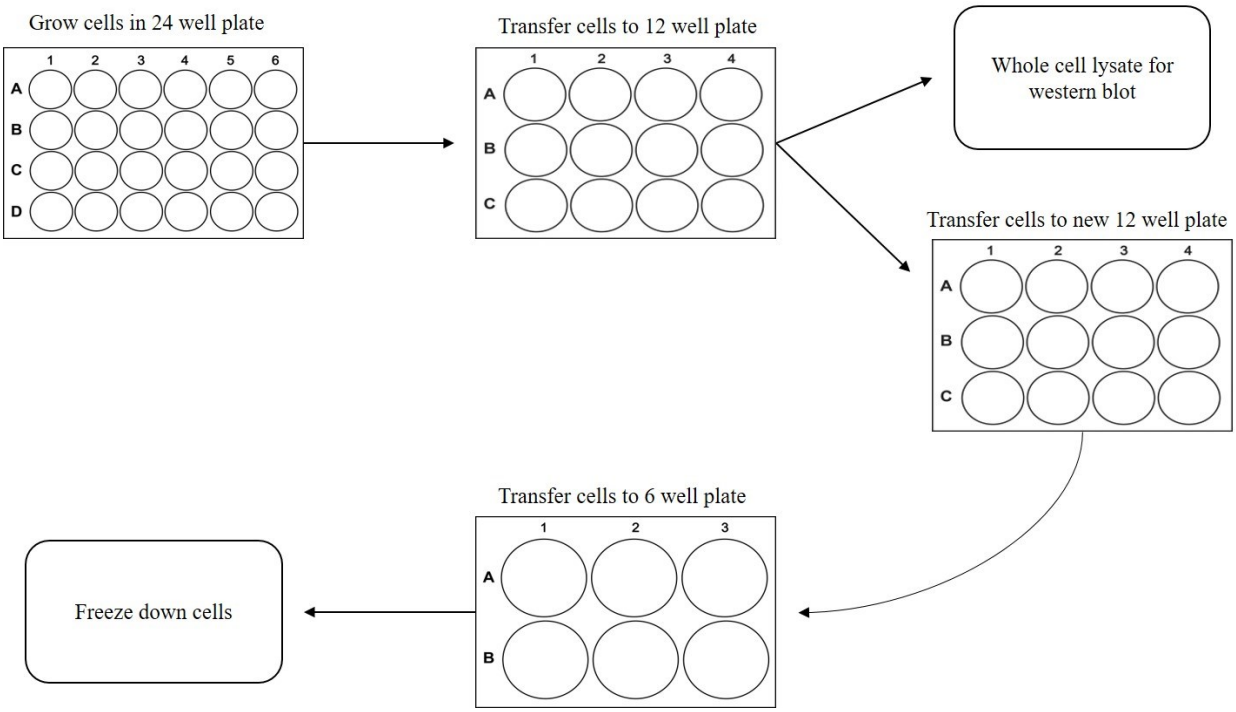

Figure 5. Depiction of the process of growing up isolated clones. Once clones were isolated from 10 cm plates, they were placed in a well of a 24-well plate and grown to confluency. As cells grew, they were transferred to each step of the flow chart.

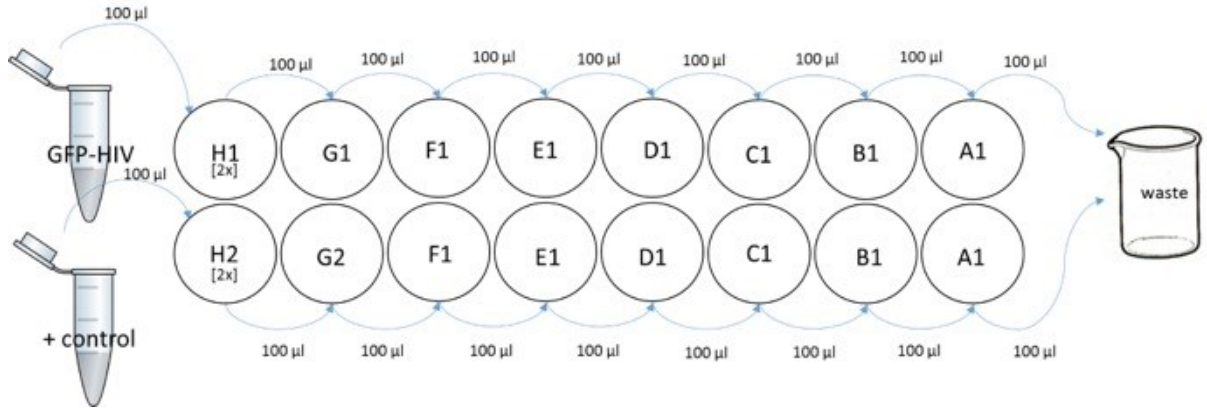

Figure 6. A depiction of how to execute the dilution series to test for infectivity of HIV-GFP. This image was created by Dr. Amy Hulme. For infection, 2X polybrene media was added to wells H1 and H2, and 1X polybrene media was added to the remaining wells (G-A). For the serial dilution, 100 µl of HIV-GFP was added to H1/H2, mixed, and then 100 µl was added to G1/G2, and the dilution proceeded in the same manner.

RESULTS

Generating C20-TC Cell Line

Hygromycin kill curve. A hygromycin kill curve was performed to establish the appropriate concentration of hygromycin to use when growing cells under selective pressure to establish a C20-TC cell line. The ideal concentration of drug would kill cells after 5 to 7 days. This timeframe allows ample time for the resistant cells to grow as well as for the drug to kill all of the cells that do not express the resistant gene. Any length of time longer than this would be inefficient when attempting to establish a cell line. Two separate experiments were done, each in a 6-well plate. The first experiment used 6 different concentrations of hygromycin, 0 µg/ml, 100 µg/ml, 200 µg/ml, 300 µg/ml, and 400 µg/ml. All cells treated with 200 µg/ml or higher died within 5 days, and cells treated with 100 µg/ml died after 6 days. These results suggest that 200 ug/ml may have been too high of a concentration of hygromycin because all of the cells died around the same time and earlier than desired. To better clarify which concentration would be best to grow cells under selective pressure, the hygromycin kill curve was repeated with lower concentrations. Cells treated with 150 µg/ml and 200 µg/ml died within 4 days, which was shorter than the desired time. Cells treated with 50 µg/ml were still alive after 6 days, which was longer than the desired length of time and it was unclear if the cells grown under these conditions would completely die off. The cells treated with 100 µg/ml died within 6 days which was within the target length of time, so this concentration of drug was chosen to use when the cell line was being generated.

Once the concentration of hygromycin was determined, C20 cells were infected with TRIM-CypA expressing virus and grown in C20 media containing 100 µg/ml of hygromycin.

After at least 6 days had passed to allow selection of hygromycin resistant cells, the cells were then diluted to establish clones from a single cell. Single colonies were picked from dilutions of 75 cells/plate and 100 cells/plate. In total 20 colonies were picked, grown, and passaged from a 24 well plate to a 12 well plate. Of the 20 colonies picked, 14 colonies survived to establish a cell line. Each of the 14 colonies were used to make a whole cell lysate sample to test each of the cell lines for presence of TRIM-CypA using a western blot.

Western blot to confirm presence of TRIM-CypA in cells. To confirm stable expression of TRIM-CypA in the newly established C20-TC cell lines, a western blot was done. A 3F10 anti-HA antibody was used to target the HA tag on TRIM-CypA. TCN14 cells were used as a positive control and had a band at 45 kDa, the correct size for TRIM-CypA (Figure 7). These cells were chosen as a positive control because they are CHME3 cells engineered to express TRIM-CypA using the same TCSH virus. As the parent cell line of TCN14, CHME3 cells were used as a negative control and had no bands (Figure 7).

Of the 14 cell lines isolated, 7 were tested for expression of TRIM-CypA and 5 were positive for TRIM-CypA expression (Figure 7). C1-5, C2-6, and C2-9 cells had the highest expression of TRIM-CypA, each with a dark band at 45 kD. C2-11 and C2-12 cells had moderately dark bands at 45 kD, but not as dark as C1-5, C2-6, and C2-9 cells. This could be due to the cells turning down expression of the TRIM-CypA gene. C1-7 and C1-8 cells had light bands near 45 kD that could be due to very low levels of expression of TRIM-CypA in the cell lines. Low levels of expression could also be due to human error while loading the wells of the gel causing some of the sample from the surrounding wells could have spilled over into the wells containing C1-7 and C1-8 samples, giving a false slightly positive result. Because they had the

best expression of TRIM-CypA, C1-5, C2-6, C2-9, C2-11, and C2-12 cell lines were chosen to continue further testing.

Infectivity of new cell lines. Infectivity assays were performed in 5 candidate cell lines to determine whether TRIM-CypA was functioning properly in the cell lines that had confirmed stable protein expression. When expressed by cells, TRIM-CypA binds to the viral capsid and blocks HIV-1 infection. CsA binds to TRIM-CypA, blocking its ability to inhibit infection. Therefore, each cell line was treated with either CsA or an EtOH control and infected with HIV-GFP virus. HIV-GFP is a green fluorescent protein (GFP) reporter virus, meaning that when HIV inserts its DNA to establish infection of the target cell, it will also insert the GFP gene. Infected cells will then express GFP, and flow cytometry is used to determine the percentage of GFP positive or infected cells. TCN14 is a cell line that stably expresses TRIM-CypA and was used as a positive control. It is expected that the TCN14 cells will have a higher infectivity in the presence of CSA and a lower infectivity in the presence of EtOH. C20 is the parent cell line that does not express TRIM-CypA and was used as a negative control. It is expected that the C20 cells will have no change of infectivity when infected with HIV-GFP in the presence and absence of CSA.

The name of each cell line tested and the infectivity of each at 1/64 dilution of virus is shown in Table 2. Infectivity at the lowest dilution of virus, 1/64, is focused on when analyzing these data because the infectivity is below 50%, which lowers the chance of 1 cell being infected by multiple viruses. For each cell line, the infectivity in the presence and absence of CsA was compared. TCN14 cells had infectivity of 15.07%-12.18% in the presence of CsA and 0.00%-0.56% in the ethanol condition, indicating that the TRIM-CypA protein was properly functioning in this cell line (Table 2). At the 1/64 dilution of virus, C20 cells had infectivity of 45.45%-

33.13% in the presence of CsA and 56.66%-50.97% in the ethanol condition, confirming that these cells did not express TRIM-CypA.

Figure 8A shows the infectivity data from the C2-9 cell line tested in the two conditions. The C2-9 cells had significantly higher percentage of GFP positive cells when infection occurred in the presence of CSA than EtOH, as expected with a functioning TRIM-CypA protein. At 1/64 dilution of virus, the C2-9 cell line infectivity was at 35.92% in comparison to 1.39% in the ethanol control. These data suggest that in the C2-9 cell line, TRIM-CypA is unable to restrict uncoating when the cells are treated with CsA but almost completely restricts infection in the ethanol control. Therefore, TRIM-CypA was properly functioning in the C2-9 cells. When compared to the TCN14 cells, TRIM-CypA in C2-9 cells was more effective. At the same dilution of virus TCN14 cells had 12.98% infectivity in CsA and 0.56% infectivity in ethanol. Although TCN14 cells had lower infectivity in ethanol at 1/64 dilution of virus, C2-9 cells had much higher infectivity in CsA. Figure 8B shows the infectivity data of C2-12 cells in the presence and absence of CsA for comparison with C2-9 cells. These cells did not show as much of a difference in infectivity in the two conditions as the C2-9 cells did. When treated with CsA, in 1/64 dilution of virus the C2-12 cells had 12.18% infected cells, which is much lower than the C2-9 cells had. In the ethanol control, C2-12 cells had 4.47% infectivity. This is much higher than the C2-9 cells and is undesirable because it indicated that TRIM-CypA is not restricting viral uncoating in as many cells as it does when expressed by the C2-9 cells. C2-9 was chosen as the cell line to use in further experiments because it had the highest infectivity in the presence of CsA and the lowest infectivity in ethanol when compared to all other cell lines, including the positive control.

Uncoating in C2-9 Cell Line

Viral titration. To accurately study HIV-1 uncoating in C20 cells, the concentration of HIV-GFP to be used in the CsA washout and viral fusion assays was determined by a viral titration. An infectivity less than 50% was desired because it lowers the probability of having more than one virus infect each individual cell, which is important because the read out of the uncoating assay and viral fusion assay is an infected cell. One infected cell represents one uncoated virus in the CsA washout assay and one fused virus in the viral fusion assay.

Two stocks of HIV-GFP, July 2017 and September 2017, were tested in a dilution series of infection in C20 cells. Figure 9 shows that the September 2017 stock of virus had higher percentages of infectivity at lower concentrations than the July 2017 stock, and was therefore chosen for future experiments. The September 2017 stock of virus was used for all experiments in this project at a 1/100 dilution. This concentration was decided based on the virus having 45.09% infectivity at 1/64 dilution and 29.79% infectivity at 1/128 dilution (Figure 9). The cells that were not treated with virus that served as a negative control did not have exactly 0.00% GFP positive cells because there was some background fluorescence in the cells detected by the flow cytometer. Once the concentration of virus to be used was determined, the CsA washout assays and viral fusion assays were performed.

CsA washout assay. To study the rate at which HIV-1 uncoats in microglial cells, the CsA washout assay was utilized in C2-9 cells. The cells were infected with HIV-GFP and treated with either CsA or the EtOH carrier control. CsA acted as a TRIM-CypA inhibitor to block the proteins ability to restrict HIV replication. The drugs were washed out at various timepoints and the percentage of GFP positive cells was determined by flow cytometry for each timepoint.

Expression of GFP by cells confirmed HIV-GFP infection and signified a successfully uncoated virus. For more accurate results, each timepoint for both conditions was performed in triplicate.

Figure 10 is representative data from one CsA washout assay. Figure 10A is the raw data graphed and Figure 10B is the data after results were normalized by subtracting the percent of GFP positive cells in the ethanol control. In Figure 10C, the highest percentage of GFP positive cells was normalized to 100% and the data was graphed. In the assays, GFP positive cells start to increase within the first hour of the experiment around 30-45 min. In the experiment, the percentage of GFP positive cells levels off at 4 hours. At 2 hours postinfection in all experiments, over half of the total GFP positive cells had uncoated virus. In Figure 10, the half-life of uncoating was calculated to be 50.2 min. From 7 experiments the average half-life of uncoating in C2-9 cells was calculated to be 65.6 min (Table 3).

Viral fusion assay. The uncoating half-lives calculated from the CsA washout assay include the timing of both viral fusion and uncoating. Viral fusion assays were conducted similarly to CsA washout assays, having the same timepoints but keeping CsA in the media and adding in a fusion inhibitor at each timepoint. At each washout timepoint, we can subtract out the timing of viral fusion using the results of a viral fusion assay that is done concurrently with the CsA washout assay. This gives a more accurate depiction of the timing of uncoating. The viral fusion assay in C2-9 cells was performed 4 times simultaneously with the CsA washout assay, using the fusion inhibitor BafA the first two experiments and NH_4Cl the last two experiments, as well as once without a CsA washout assay. Each timepoint for each experiment was performed in triplicate, and the standard error for each is shown on the graphs. Representative data from one viral fusion assay is shown in Figure 11. Figure 11A is the raw data from the experiment and

Figure 11B is the data normalized to 0% fusion at the 0 hr timepoint. Figure 11C is the data with the highest percentage of GFP positive cells normalized to 100%.

The average half-lives calculated from 4 viral fusion assays done concurrently with washouts was 40.9 min (Table 4). In comparison, the average uncoating half-life from these experiments was 63.3 min and the average difference between the uncoating half-life and viral fusion half-life was 22.3 min (Table 4). To compare the parent cell line with the newly established, TRIM-CypA expressing cell line, 2 fusion assays were performed simultaneously with C20 and C2-9 cells. From the 2 experiments shown in data Table 5, the average half-live of fusion in the C20 cells was 79.5 min and in the C2-9 cells was 63.3 min. The newly established cell line was found to fuse faster than the parent cell line.

Effect of CsA in the C20 cell line. It was important to understand how CsA influenced overall infectivity in C2-9 cells because viral uncoating was studied in cells that were treated with this drug. C2-9 cells express TRIM-CypA and require CsA present for viral uncoating to occur in the cells, so it is impossible to study infectivity of the cells with CsA present and absent. Therefore, the C20 parent cell line of C2-9 was used in this investigation. To test infectivity, a serial dilution of virus was used to infect C20 cells in CsA and in an ethanol control. The experiment was repeated 3 times to ensure accuracy. As shown in Figure 12, it was observed that infectivity was slightly decreased in the presence of CsA when compared to ethanol. Average infectivity of the 3 experiments when 1/64 diluted virus was used to infect C20 cells treated with CsA was 4.54% while the same dilution of virus used to infect C20 cells treated with ethanol resulted in an average of 12.78% infectivity (Table 6). This could be due to CsA binding to host protein CypA and inhibiting the interaction between CypA and viral capsid. At dilutions of virus near ½, conclusions cannot be drawn because there is a higher probability that more than one

virus infects one cell. Because the read out of the assay is one infected cell, there is no way to tell whether the results at these lower dilutions accurately represent the amount of established infection.

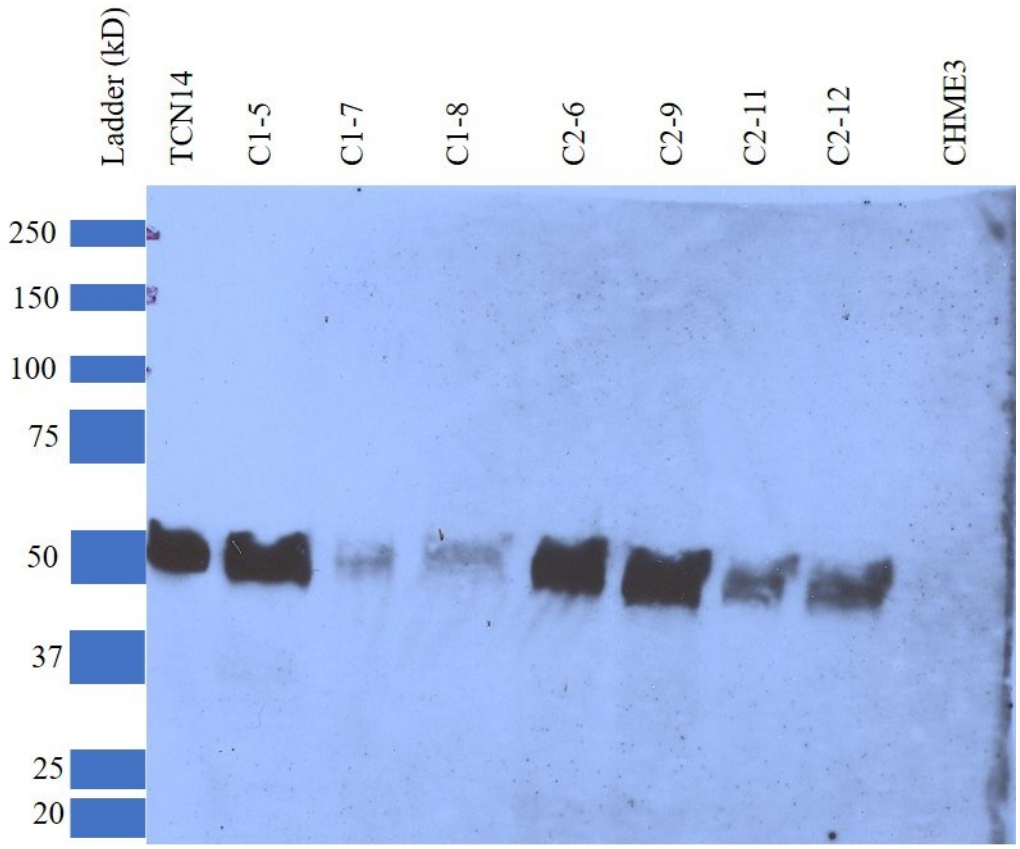

Figure 7. Western blot to confirm presence of TRIM-CypA in new cell lines. 7 of the 14 cell lines were analyzed by Western Blot using a primary anti-HA antibody targeting the HA tag on TRIM-CypA. A standard protein ladder (Bio-Rad) was used. TCN14 cells, which are CHME3 cells engineered to express TRIM-CypA, served as a positive control and CHME3 cells served as a negative control. The new cell lines under investigation were C1-5, C1-7, C1-8, C2-6, C2-9, C2-11, and C2-12.

A

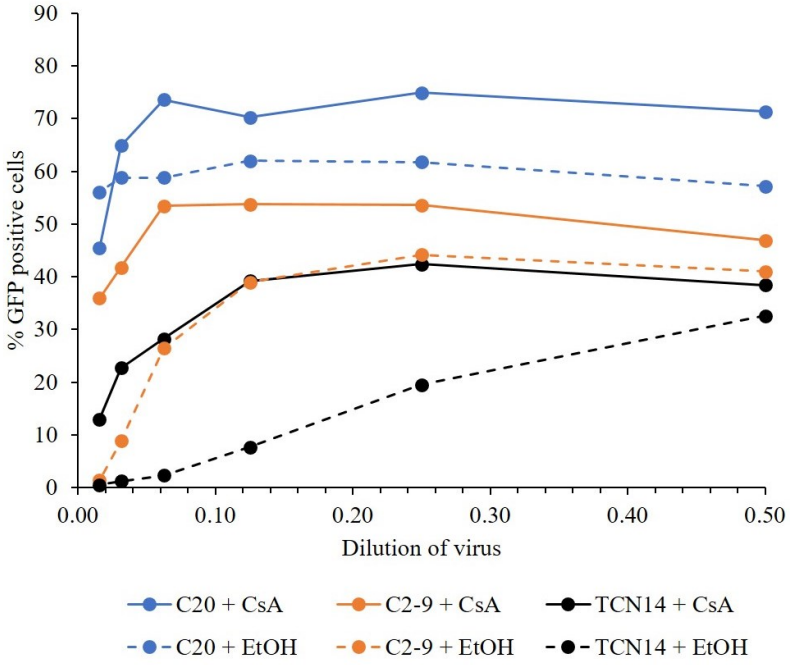

B

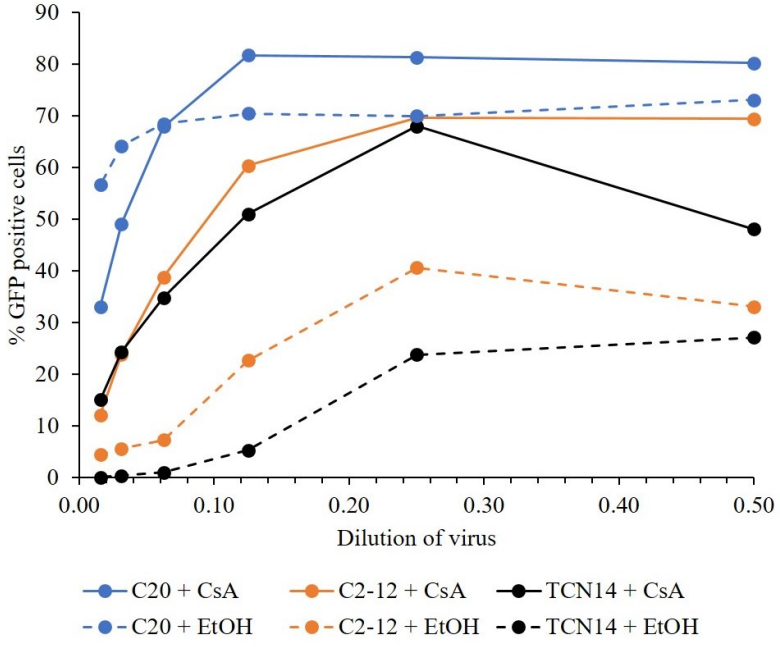

Figure 8. Infectivity of the new cell lines compared to C20 and TCN14 cell lines in the presence and absence of CsA. Infectivity assays were performed in seven chosen new cell lines (C1-5, C2-6, C2-6, C2-11, C2-12) to determine what effect CsA had on overall HIV-GFP infectivity of the cell line. The assays were conducted using the TCN14 cell line as a positive control and the C20 cell line as a negative control. A) Results of the infectivity assay with C2-9, C20, and TCN14 cells. B) Results of the infectivity assay with C2-12, C20, and TCN14 cells.

Table 2. Infectivity of new cell lines with 1/64 dilution of virus in the presence and absence of CsA. To study how effective TRIM-CypA was in each newly established cell line, the cells were infected with HIV-GFP and treated with CsA, and the viral infectivity was compared to an ethanol control. A dilution of 1/64 was used for comparison because infectivity of the cells at this dilution was below 50%, lowering the probability of one cell being infected by more than one virus. The range of the results for each control, TCN14 and C20, is shown as these cell lines were tested multiple times, once with each new cell line, whereas the new cell lines were only tested once.

	% GFP positive cells	
Cell line	CsA	EtOH
C1-5	13.30	0.21
C2-6	31.35	1.66
C2-9	35.92	1.39
C2-11	13.85	1.15
C2-12	12.18	4.47
TCN14	12.18-15.07	0.00-0.56
C20	33.13-45.45	50.97-56.66

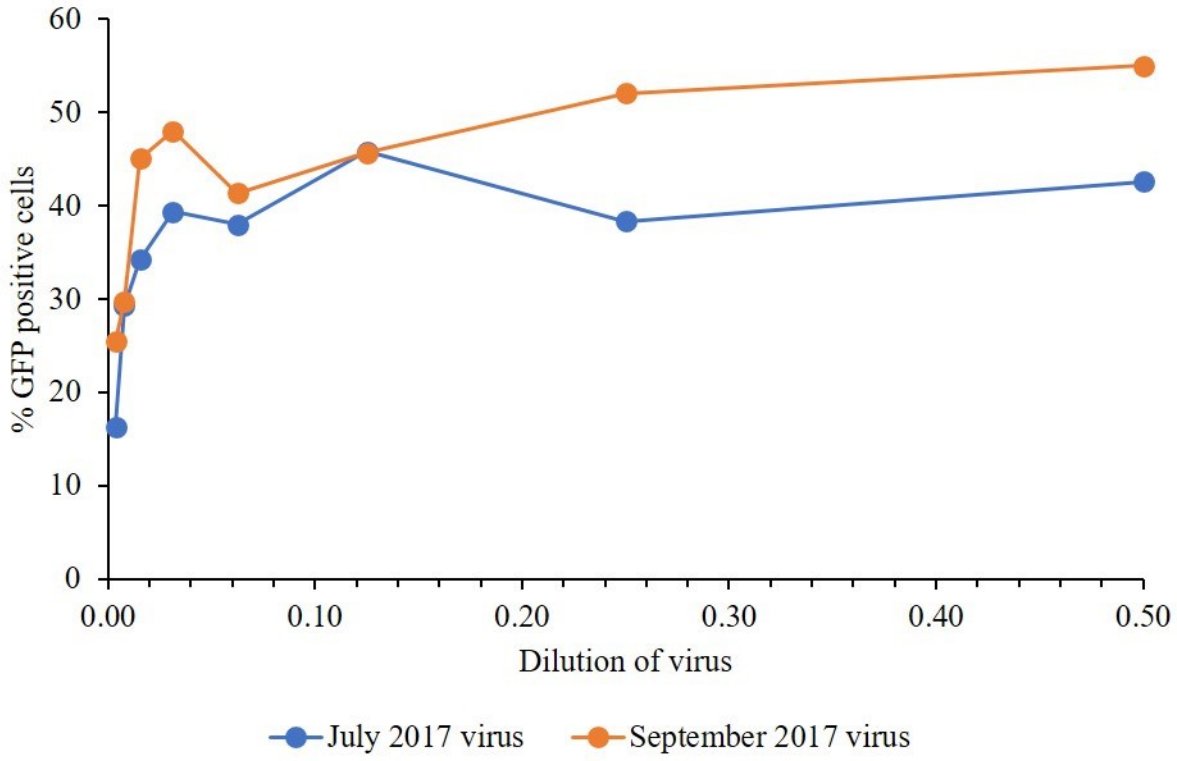

Figure 9. Dilution series of HIV-GFP virus stock. Two stocks of HIV-GFP virus, July 2017 and September 2017, were used to infect C20 cells at sequential dilutions to help determine the most suitable dilution of virus to use in future experiments.

A

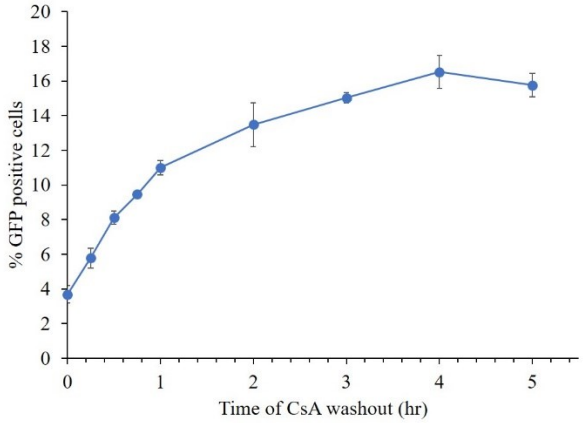

B

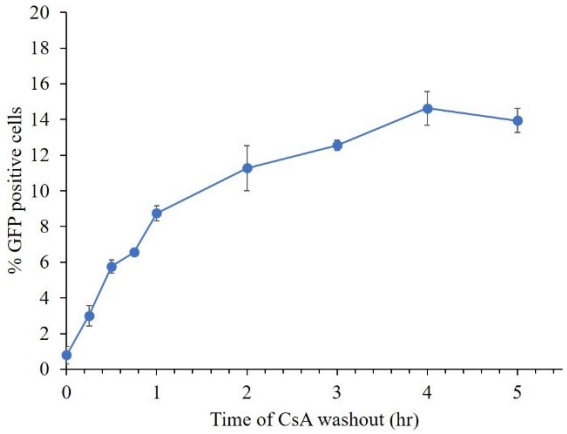

C

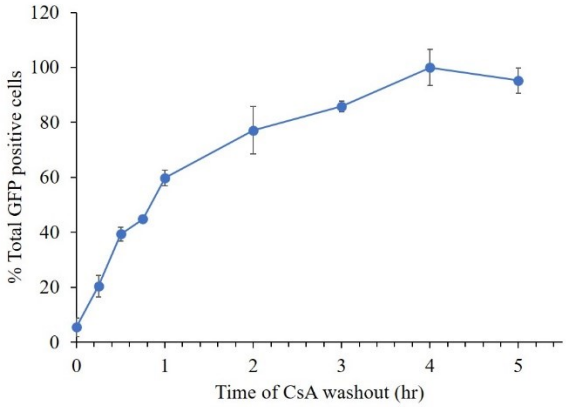

Figure 10. A representative CsA washout assay. Data from the experiment on 12/14/2018 were chosen to represent all 7 of the CsA washout assays conducted because of the high percentage of living cells and an ideal ethanol control. A) Raw data results. B) Results after being normalized by subtracting the percentage of GFP positive cells in the ethanol control. C) Data graphed after the results were normalized by setting the highest percentage of GFP positive cells at 100%.

Table 3. CsA washout assays conducted with and without collecting viral fusion data. In each experiment, C2-9 cells were infected with HIV-GFP in the presence of CsA or an ethanol control, and the percentage of infected cells was determined by GFP fluorescence. Some CsA washout assays were performed side-by-side with viral fusion assays, while others were not.

Date	Uncoating half-life (min)	Viral fusion data collected
09/27/18	64.2	No
10/04/18	85.1	No
10/10/18	117.3	Yes
11/03/18	58.3	Yes
11/12/18	56.4	No
12/05/18	27.4	Yes
12/14/18	50.2	Yes
Average	65.6	

A

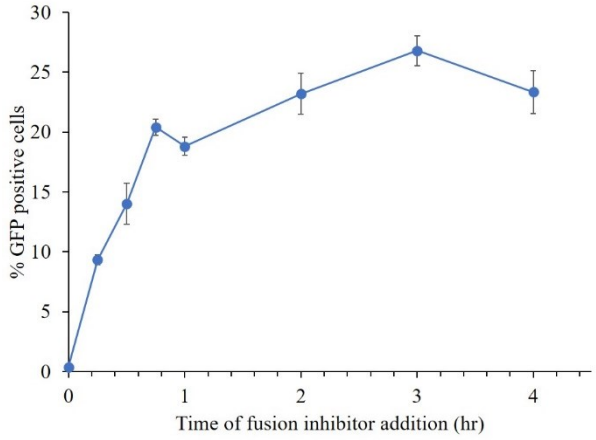

B

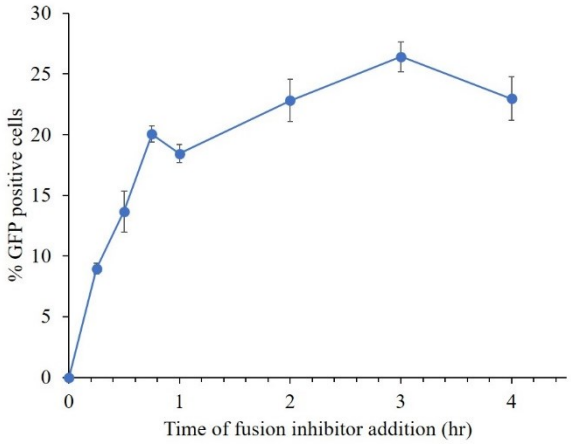

C

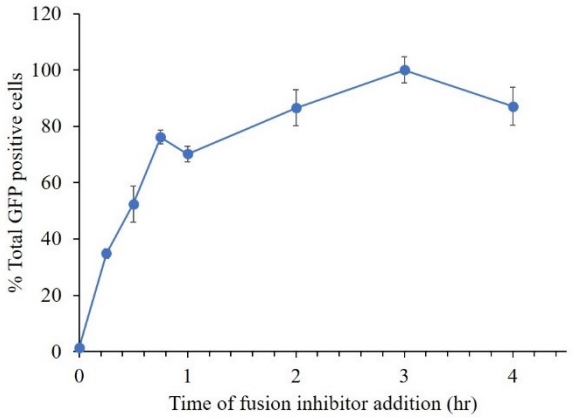

Figure 11. A representative viral fusion assay. Data from the experiment on 12/14/18 were chosen to represent all 5 viral fusion assays conducted because of the ideal number of living cells. A) Raw data. B) Data after the results were normalized to 0% GFP positive cells at the 0 hr timepoint. C) Results after the highest percentage of GFP positive cells was normalized to 100%.

Table 4. Side-by-side CsA washout and viral fusion assays**.** These assays were conducted with the same timepoints at the same time to study the rate of uncoating while accounting for the timing of viral fusion and holding conditions such as cellular and environmental factors constant.

Date	Fusion half-life (min)	Uncoating half-life (min)	Difference (min)
10/10/18	89.6	117.3	27.7
11/03/18	23.6	58.3	34.7
12/05/18	21.9	27.4	5.5
12/14/18	28.8	50.2	21.4
Average	40.9	63.3	22.3
Standard error	16.3	19.2	

Table 5. Viral fusion assays that were conducted in C20 and C2-9 cells. These assays were conducted to compare the rate of viral fusion in C2-9 cells and the parent cell line, C20.

Date	Fusion C2-9 half-life (min)	Fusion C20 half-life (min)
09/10/18	36.9	67.9
10/10/18	89.6	91.1
Average	63.3	79.5

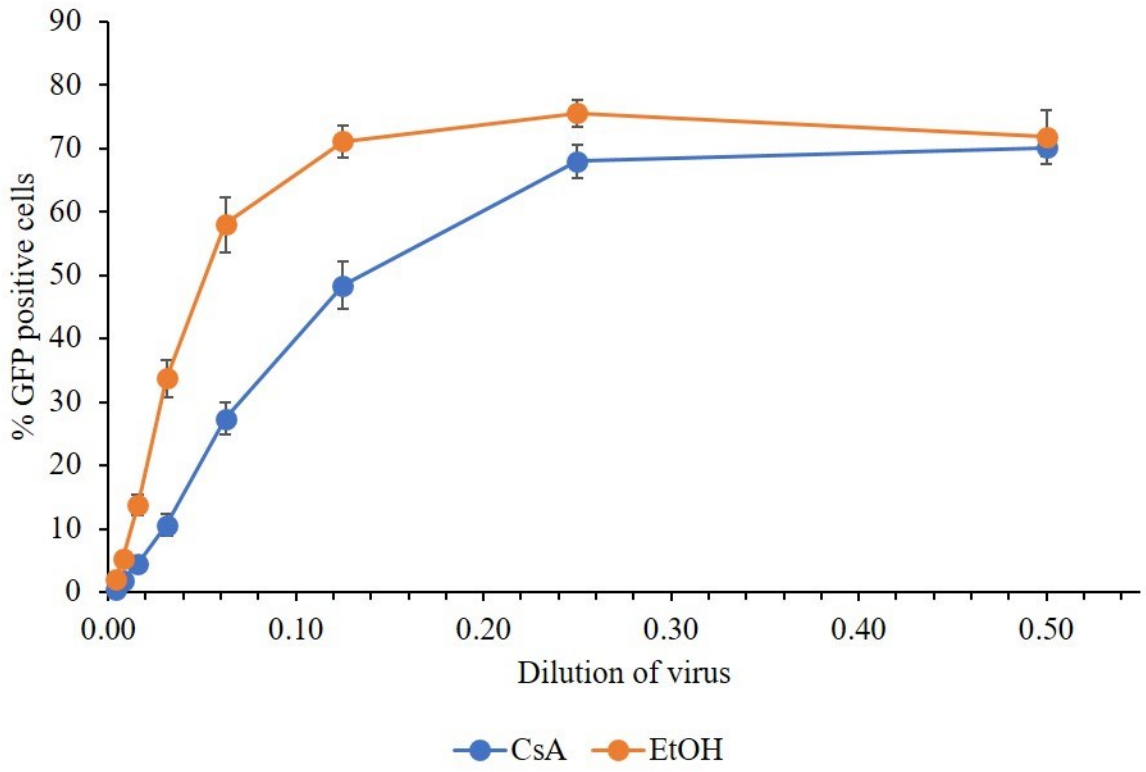

Figure 12. The effect of CsA on HIV-GFP infectivity in C20 cells**.** The data from the infectivity assay conducted on 02/09/18 was used to create a representative graph for all of the experiments. C20 cells were infected with different dilutions of HIV-GFP in the presence of CsA or an ethanol control. The percentage of infected cells was determined by percentage of GFP positive cells.

Table 6. The effect of CsA on 1/64 dilution of HIV-GFP in C20 cells. The infectivity of different dilutions of HIV-GFP was tested in the presence and absence of CsA to determine the effect of CsA on infectivity. The dilution of 1/64 was used during analytics to ensure accuracy.

Date	Avg. % GFP positive cells in CsA	Avg. % GFP positive cells in EtOH
02/05/18	4.08	11.11
02/09/18	4.53	13.83
03/08/18	5.02	11.72
Average	4.54	12.78

DISCUSSION

CsA washout assays have been used to study uncoating kinetics in various cell lines including Owl Monkey Kidney (OMK) cells, a TRIM-CypA expressing HeLa cell line (HeLa-TC), and now a TRIM-CypA expressing microglial cell line (C2-9). C2-9 cells had an average uncoating half-life of 63.3 min, while other studies found the uncoating half-life was near 64 min in OMK cells and 37 min in HeLa-TC cells (Table 4; Hulme et al., 2015). The timing of viral fusion is essential to consider when comparing uncoating half-lives to ensure that a discrepancy in uncoating kinetics is not due to delayed or accelerated viral fusion. The average fusion half-life in C2-9 cells was 40.9 min, in OMK cells was near 19 min, and in HeLa-TC cells was near 28 min (Table 4; Hulme et al., 2015). Virus in OMK cells fused faster than the C2-9 and HeLa-TC cells, yet virus in OMK cells uncoated slower than in the C2-9 and HeLa-TC cells. This information confirms that the delay of uncoating observed in OMK cells was not due to a delay in viral fusion. When subtracting the average half-life of viral fusion from the average uncoating half-life, the difference was 22 min in C2-9 cells, 45 min in OMK cells, and 9 min in HeLa-TC cells (Table 4; Hulme et al., 2015). It is not surprising that the timing of uncoating in C2-9 cells is more similar to HeLa-TC cells than OMK cells because HeLa cells are a human cell line while OMK cells are not.

An *in situ* uncoating assay in C2-9 cells would be an alternative way to confirm the rate of uncoating and viral fusion of HIV-1 in microglial cells (Yamashita et al., 2007). This assay uses a dual fluorescently labeled virus containing GFP-Vpr to visualize all virions and S15-mCherry to visualize virions that have not yet fused, as well as CA staining to determine if uncoating has occurred. At different timepoints post-infection, cells are stained for CA protein

using an anti-CA primary antibody and a fluorescently labeled secondary antibody (Yamashita et al., 2007). The cells are imaged to determine the amount of GFP positive virions for each timepoint. These virions are then examined for S15-mCherry signal, expressed by unfused virus, and CA protein signal, expressed by viral complexes that have not yet uncoated (Yamashita et al., 2007). Data collected from this assay can determine the amount of fusion and uncoating that occurs over time. In C2-9 cells, it is expected that the number of fused GFP-Vpr positive particles would significantly increase between 30 min and 1 hr, and the number of particles positive for CA staining would significantly decrease at approximately 1 hr as uncoating occurs.

The *in situ* uncoating assay is performed *in vivo*, like the CsA washout assay, and would therefore produce data that is easily comparable to the data obtained in this study. The benefit of conducting both the CsA washout assay and the *in situ* uncoating assay in C2-9 cells is obtaining data regarding uncoating using different methods with different benefits. The CsA washout assay read out is one infected cell, which removes any replication incompetent virus that the *in situ* assay includes. The CsA washout assay is conducted in living cells over time, allowing viral replication to run its course, which may provide more beneficial data than the *in situ* assay that fixes cells at various timepoints. A benefit for the *in situ* uncoating assay is the ability to directly visualize CA protein to see coated and uncoated virions in each individual cell. This assay directly detects CA protein while the CsA washout assay uses the ability of TRIM-CypA to restrict infection as an indirect method to detect CA.

The variation in the CsA washout results seen in this study is most likely due to a change in cellular environment (Table 4). Minor changes in the execution of each experiment such as how long the cells incubated at 16°C following spinoculation could slightly influence results. Specific bottles of media used, the amount of time cells were in culture, and the exact

temperature of reagents could also cause a variation in kinetics of steps of viral infectivity in cells. There was an attempt to control all confounding variables by conducting all runs of the same experiments within a reasonable amount of time, around 2 months, and making note to use the same bottle of media if possible. Reagents were used and stored in the same manner each experiment in an attempt to decrease any chance that reagents may have an unintentional effect on experimental results. The timing of the steps of HIV-GFP infectivity in cells is dependent on viral and cellular factors, which could change with the environment. To account for variation, each timepoint is done in triplicate and the assay was run 7 times.

Cellular factors may also contribute to the differences observed in viral fusion and uncoating kinetics in OMK, C2-9, and HeLa-TC cells. Cellular factors may be expressed in one cell line at a different rate than the others. For example, the microtubule motor protein KIF5B has been shown to mediate uncoating in cooperation with NUP358 in HeLa cells and monocyte derived macrophages (Dharan et al., 2016). To determine if the level of expression of KIF5B has an effect on the kinetics of uncoating, this cellular factor could be investigated in OMK, C2-9, and HeLa cells. To examine the expression of KIF5B in each cell line, quantitative PCR (qPCR) could be utilized to quantify expression. I would expect to see a significant difference in expression of this protein when comparing the human cell lines, C2-9 and HeLa-TC, to the OMK cells because they originate from different species and have differing uncoating kinetics. A proximal ligation assay could be utilized with antibodies specific to KIF5B and CA protein to determine if this cellular factor interacts directly or indirectly with the capsid in each cell line (Dharan et al., 2016). From this assay, I would expect to see KIF5B interacting directly with the viral capsid in human cell lines, which would produce many fluorescent puncta as the antibodies associated with KIF5B and CA interact. This finding could attribute the faster uncoating kinetics

observed in these cells to KIF5B. In OMK cells, an indirect interaction between KIF5B and CA protein would be expected and marked by a lack of fluorescent puncta leading to delayed uncoating observed in these cells. If the expression of KIF5B and the interaction of KIF5B with CA protein differs as I am suggesting, then this molecule could be a cellular factor that contributes to the difference of uncoating kinetics seen in the human cell lines and OMK cells.

To determine which model of uncoating is most likely, it is important to compare the timing of viral fusion and uncoating to estimate how quickly after fusion a virus uncoats. In the side-by-side assays, the average half-life of viral fusion was 40.9 min and the average half-life of uncoating was 63.3 min (Table 4). These data discredit the likelihood of the rapid uncoating model because if virus rapidly uncoated immediately following viral fusion, the half-life of uncoating would be only minutes longer than the half-life of viral fusion. The rapid uncoating model has been widely discredited in the field because of overwhelming evidence of CA present in the cytoplasm associated with RTC and cellular host factors (McDonald et al., 2002; Peng et al., 2014). Because there is a calculated uncoating half-life of 22.3 min when the half-life of viral fusion is accounted for, the cytoplasmic uncoating model or nuclear pore complex model of uncoating is more likely with these data (Table 4). Experimentation in HeLa cells discovered an approximate nuclear import time of 4.3 hours postinfection (± 2.6) using live cell imaging to visualize the nuclear import of fluorescently labeled virions by staining the nuclear membrane (Burdick et al., 2017). When the average uncoating half-life of HeLa cells of 37 min is taken into consideration with this nuclear import time, the cytoplasmic uncoating model seems to be more likely than the nuclear pore complex model.

In C2-9 cells, assays measuring nuclear import kinetics would help determine when uncoating occurs in relation to nuclear import to help differentiate between uncoating models. To

do this, an *in situ* uncoating experiment could be performed that includes staining the nucleus like that was done in the HeLa cells (Burdick et al., 2017). This assay would be advantageous because of the ability to visualize both coated and uncoated viral complexes in relation to the nucleus. Using images from this assay, it may be possible to distinguish between the cytoplasmic uncoating model and nuclear pore complex uncoating model by staining the nucleus and considering the distance between coated virions and the nucleus before the intact capsid undergoes uncoating. Another way to determine nuclear import kinetics is by measuring the amount of 2-LTR circular viral DNA. These DNA complexes form only after synthesis of linear viral DNA and nuclear import, likely because the nucleus provides the necessary environment for circularization of retroviral DNA (Withers-Ward, Kitamura, Barnes, & Coffin, 1994). The method of qPCR can be used to quantify 2-LTR products at different timepoints post-infection using primers specific to this product (Butler, Hansen, & Bushman, 2001). The number of 2-LTR products at each timepoint would signify the amount of nuclear import that has occurred by that time post-infection. This method could be utilized to investigate the kinetics of nuclear import in C2-9 cells as it is specific and rapid, but it does not offer the ability to visualize a virion entering the nucleus like fluorescence microscopy does. If uncoating occurs in C2-9 cells following the cytoplasmic uncoating model, images from the *in situ* staining assay would show a considerable amount of distance between coated virions and the nucleus, and qPCR would produce results in which there would be a large increase of 2-LTR copies observed at a post-infection timepoint much later than 1 hr, as the established half-life of uncoating in C2-9 cells is 63.3 min (Table 4). If the nuclear pore complex model is more characteristic of uncoating in these cells, then images from the *in situ* staining experiment would show negligible distance between the coated virions and nucleus, and qPCR would show a large increase in 2-LTR copies near the 1 hr post-infection

timepoint. The results from images obtained from the *in situ* assays combined with the kinetics of uncoating and nuclear import could potentially be enough evidence to conclude which model of uncoating occurs in C2-9 cells.

Repeating assays that measure fusion, uncoating, and nuclear import in different cell types could help decipher if uncoating follows different models in different cell types. The focus of these experiments should be cells that express a CD4 receptor on their surface and are therefore natural targets of HIV-1. Uncoating kinetics have been characterized in the microglial cell line CHME3 using the TRIM-CypA expressing daughter cell line TCN14 and now in a microglial cell line that is more characteristic of primary microglial cells, C20, using the TRIM-CypA expressing daughter cell line C2-9 (Hulme, 2019). The next cell type to be tested could be dendritic cells, as they function as a messenger in the immune system and express CD4, making them a natural HIV-1 target. To test dendritic cells, the human monocytic cell line THP-1 can be differentiated into mature dendritic cells when cultured into serum free-media containing GM-CSF, TNF-alpha, and ionomycin (Berges et al., 2005). This cell line derived from human monocytes is ideal to use in this investigation simply because it originates from humans, which are the focus of this HIV-1 study.

Virus with mutated capsid is used to study the role that CA protein has in HIV-1 uncoating and infectivity. The rate of uncoating is important to study because it effects overall viral infectivity. A92E is a CypA restricted mutant that significantly increases the rate of uncoating and has a decrease of infectivity (Hulme et al., 2015; Qi, Yang, & Aiken, 2008). E45A is a mutant that increases capsid core stability, delays uncoating and also has a decrease of infectivity (Hulme et al., 2015; von Schwelder et al., 2003). Mutant N74D was found to delay uncoating, even more so in HeLa-TC cells than in OMK cells, and has a decrease of infectivity

(Ambrose et al., 2012; Hulme et al., 2015). The difference in severity of delay of uncoating with mutant N74D further supports the hypothesis that the difference of cellular environment in the HeLa-TC cells and OMK cells has an effect on HIV-1 uncoating. It would be beneficial to conduct CsA washout assays in C2-9 cells with capsid mutants in the future to investigate how the environment of this cell line interacts with CA protein and what effect that has on uncoating. Data collected could be compared to the previously reported data on capsid mutants in OMK and HeLa-TC cells, and any differences in the kinetics of uncoating of capsid mutant virus may implicate cellular factors that are different among these cell lines. New cellular factors could be potentially identified by discerning any differences in the kinetics of uncoating of mutant virus between the cell lines and comparing global gene expression of the cell lines.

From the use of capsid mutant virus, it appears that if uncoating occurs at a faster or slower rate than the wild type rate then infectivity is decreased. This makes the step of uncoating a point of interest when considering potential drug targets with the aim of decreasing viral infectivity. There are currently no antiretroviral pharmaceuticals designed to target the step of uncoating. BI-2 and PF74 are drugs that use similar mechanisms to bind to the capsid to block HIV-1 infection and are often used in research but were discontinued during pharmaceutical development (Fricke, Buffone, Opp, Valle-Casuso, & Diaz-Griffero, 2014; Shi, Zhou, Shah, Aiken, & Whitby, 2010). As more research is done on uncoating, it is hoped that this step of viral replication can serve as a new drug target that is used to improve the lives of those affected by HIV-1.

REFERENCES

Accola, M. A., Öhagen, Å., & Göttlinger, H. G. (2000). Isolation of Human Immunodeficiency Virus Type 1 Cores: Retention of Vpr in the Absence of p6 gag. *Journal of Virology*, *74*(13), 6198–6202. https://doi.org/10.1128/JVI.74.13.6198-6202.2000

Ambrose, Z., Lee, K., Ndjomou, J., Xu, H., Oztop, I., Matous, J., … KewalRamani, V. N. (2012). Human immunodeficiency virus type 1 capsid mutation N74D alters cyclophilin A dependence and impairs macrophage infection. *Journal of Virology*, *86*(8), 4708–4714. https://doi.org/10.1128/JVI.05887-11

Berges, C., Naujokat, C., Tinapp, S., Wieczorek, H., Höh, A., Sadeghi, M., … Daniel, V. (2005). A cell line model for the differentiation of human dendritic cells. *Biochemical and Biophysical Research Communications*, *333*(3), 896–907. https://doi.org/10.1016/j.bbrc.2005.05.171

Berthet-Colominas, C., Monaco, S., Novelli, A., Sibaï, G., Mallet, F., & Cusack, S. (1999). Head-to-tail dimers and interdomain flexibility revealed by the crystal structure of HIV-1 capsid protein (p24) complexed with a monoclonal antibody Fab. *The EMBO Journal*, *18*(5), 1124–1136. https://doi.org/10.1093/emboj/18.5.1124

Bhattacharya, A., Alam, S. L., Fricke, T., Zadrozny, K., Sedzicki, J., Taylor, A. B., … Yeager, M. (2014). Structural basis of HIV-1 capsid recognition by PF74 and CPSF6. *Proceedings of the National Academy of Sciences of the United States of America*, *111*(52), 18625–18630. https://doi.org/10.1073/pnas.1419945112

Blankson, J. N., Persaud, D., & Siliciano, R. F. (2002). The challenge of viral reservoirs in HIV-1 infection. *Annual Review of Medicine*, *53*, 557–593. https://doi.org/10.1146/annurev.med.53.082901.104024

Bosco, D. A., Eisenmesser, E. Z., Pochapsky, S., Sundquist, W. I., & Kern, D. (2002). Catalysis of cis/trans isomerization in native HIV-1 capsid by human cyclophilin A. *Proceedings of the National Academy of Sciences of the United States of America*, *99*(8), 5247–5252. https://doi.org/10.1073/pnas.082100499

Brass, A. L., Dykxhoorn, D. M., Benita, Y., Yan, N., Engelman, A., Xavier, R. J., … Elledge, S. J. (2008). Identification of host proteins required for HIV infection through a functional genomic screen. *Science*, *319*(5865), 921–926. https://doi.org/10.1126/science.1152725

Briggs, J. A. G., Simon, M. N., Gross, I., Kräusslich, H.-G., Fuller, S. D., Vogt, V. M., & Johnson, M. C. (2004). The stoichiometry of Gag protein in HIV-1. *Nature Structural & Molecular Biology*, *11*(7), 672–675. https://doi.org/10.1038/nsmb785

Briones, M. S., Dobard, C. W., & Chow, S. A. (2010). Role of human immunodeficiency virus type 1 integrase in uncoating of the viral core. *Journal of Virology*, *84*(10), 5181–5190. https://doi.org/10.1128/JVI.02382-09

Burdick, R. C., Delviks-Frankenberry, K. A., Chen, J., Janaka, S. K., Sastri, J., Hu, W.-S., & Pathak, V. K. (2017). Dynamics and regulation of nuclear import and nuclear movements of HIV-1 complexes. *PLoS Pathogens*, *13*(8), e1006570. https://doi.org/10.1371/journal.ppat.1006570

Butler, S. L., Hansen, M. S., & Bushman, F. D. (2001). A quantitative assay for HIV DNA integration in vivo. *Nature Medicine*, *7*(5), 631–634. https://doi.org/10.1038/87979

Campbell, E. M., & Hope, T. J. (2015). HIV-1 capsid: the multifaceted key player in HIV-1 infection. *Nature Reviews. Microbiology*, *13*(8), 471–483. https://doi.org/10.1038/nrmicro3503

Campbell, E. M., Perez, O., Melar, M., & Hope, T. J. (2007). Labeling HIV-1 virions with two fluorescent proteins allows identification of virions that have productively entered the target cell. *Virology*, *360*(2), 286–293. https://doi.org/10.1016/j.virol.2006.10.025

Centers for Disease Control and Prevention. (2019a). HIV Transmission. Retrieved from https://www.cdc.gov/hiv/basics/transmission.html

Centers for Disease Control and Prevention. (2019b). PEP. Retrieved from https://www.cdc.gov/hiv/basics/pep.html

Centers for Disease Control and Prevention. (2019c). PrEP. Retrieved from https://www.cdc.gov/hiv/basics/prep.html

Checkley, M. A., Luttge, B. G., & Freed, E. O. (2011). HIV-1 envelope glycoprotein biosynthesis, trafficking, and incorporation. *Journal of Molecular Biology*, *410*(4), 582–608. https://doi.org/10.1016/j.jmb.2011.04.042

Cosnefroy, O., Murray, P. J., & Bishop, K. N. (2016). HIV-1 capsid uncoating initiates after the first strand transfer of reverse transcription. *Retrovirology*, *13*(1), 58. https://doi.org/10.1186/s12977-016-0292-7

Delaney, M. K., Malikov, V., Chai, Q., Zhao, G., & Naghavi, M. H. (2017). Distinct functions of diaphanous-related formins regulate HIV-1 uncoating and transport. *Proceedings of the National Academy of Sciences of the United States of America*, *114*(33), E6932–E6941. https://doi.org/10.1073/pnas.1700247114

Dharan, A., Opp, S., Abdel-Rahim, O., Keceli, S. K., Imam, S., Diaz-Griffero, F., & Campbell, E. M. (2017). Bicaudal D2 facilitates the cytoplasmic trafficking and nuclear import of HIV-1 genomes during infection. *Proceedings of the National Academy of Sciences of the United States of America*, *114*(50), E10707–E10716. https://doi.org/10.1073/pnas.1712033114

Dharan, A., Talley, S., Tripathi, A., Mamede, J. I., Majetschak, M., Hope, T. J., & Campbell, E. M. (2016). KIF5B and Nup358 Cooperatively Mediate the Nuclear Import of HIV-1 during Infection. *PLoS Pathogens*, *12*(6), e1005700. https://doi.org/10.1371/journal.ppat.1005700

Dismuke, D. J., & Aiken, C. (2006). Evidence for a functional link between uncoating of the human immunodeficiency virus type 1 core and nuclear import of the viral preintegration complex. *Journal of Virology*, *80*(8), 3712–3720. https://doi.org/10.1128/JVI.80.8.3712-3720.2006

Elbirt, D., Mahlab-Guri, K., Bazalel-Rosenberg, S., Gill, H., Attali, M., & Asher, I. (2015). HIV-Associated Neurocognitive Disorders (HAND). *Saturday Review*, *9*, 19. Retrieved from https://pdfs.semanticscholar.org/4377/7e506007b20f6d0e79e04837c0fbf3a30c9f.pdf

Fassati, A., & Goff, S. P. (2001). Characterization of intracellular reverse transcription complexes of human immunodeficiency virus type 1. *Journal of Virology*, *75*(8), 3626–3635. https://doi.org/10.1128/JVI.75.8.3626-3635.2001

Forshey, B. M., von Schwedler, U., Sundquist, W. I., & Aiken, C. (2002). Formation of a human immunodeficiency virus type 1 core of optimal stability is crucial for viral replication. *Journal of Virology*, *76*(11), 5667–5677. Retrieved from https://www.ncbi.nlm.nih.gov/pubmed/11991995

Frankel, A. D., & Young, J. A. (1998). HIV-1: fifteen proteins and an RNA. *Annual Review of Biochemistry*, *67*, 1–25. https://doi.org/10.1146/annurev.biochem.67.1.1

Freed, E. O. (2001). HIV-1 replication. *Somatic Cell and Molecular Genetics*, *26*(1-6), 13–33. Retrieved from https://www.ncbi.nlm.nih.gov/pubmed/12465460

Fricke, T., Brandariz-Nuñez, A., Wang, X., Smith, A. B., 3rd, & Diaz-Griffero, F. (2013). Human cytosolic extracts stabilize the HIV-1 core. *Journal of Virology*, *87*(19), 10587–10597. https://doi.org/10.1128/JVI.01705-13

Fricke, T., Buffone, C., Opp, S., Valle-Casuso, J., & Diaz-Griffero, F. (2014). BI-2 destabilizes HIV-1 cores during infection and Prevents Binding of CPSF6 to the HIV-1 Capsid. *Retrovirology*, *11*, 120. https://doi.org/10.1186/s12977-014-0120-x

Garcia-Mesa, Y., Jay, T. R., Checkley, M. A., Luttge, B., Dobrowolski, C., Valadkhan, S., … Alvarez-Carbonell, D. (2017). Immortalization of primary microglia: a new platform to study HIV regulation in the central nervous system. *Journal of Neurovirology*, *23*(1), 47–66. https://doi.org/10.1007/s13365-016-0499-3

Gaudin, R., de Alencar, B. C., Arhel, N., & Benaroch, P. (2013). HIV trafficking in host cells: motors wanted! *Trends in Cell Biology*, *23*(12), 652–662. https://doi.org/10.1016/j.tcb.2013.09.004

Hatziioannou, T., Perez-Caballero, D., Cowan, S., & Bieniasz, P. D. (2005). Cyclophilin interactions with incoming human immunodeficiency virus type 1 capsids with opposing effects on infectivity in human cells. *Journal of Virology*, *79*(1), 176–183. https://doi.org/10.1128/JVI.79.1.176-183.2005

Hulme, A. E. (2019). *Characterization of HIV-1 uncoating in a human microglial cell line.* Unpublished manuscript, Missouri State University, Springfield, MO.

Hulme, A. E., & Hope, T. J. (2014). The cyclosporin A washout assay to detect HIV-1 uncoating in infected cells. *Methods in Molecular Biology*, *1087*, 37–46. https://doi.org/10.1007/978-1-62703-670-2_4

Hulme, A. E., Kelley, Z., Okocha, E. A., & Hope, T. J. (2015). Identification of capsid mutations that alter the rate of HIV-1 uncoating in infected cells. *Journal of Virology*, *89*(1), 643–651. https://doi.org/10.1128/JVI.03043-14

Hulme, A. E., Perez, O., & Hope, T. J. (2011). Complementary assays reveal a relationship between HIV-1 uncoating and reverse transcription. *Proceedings of the National Academy of Sciences of the United States of America*, *108*(24), 9975–9980. https://doi.org/10.1073/pnas.1014522108

Janabi, N., Peudenier, S., Héron, B., Ng, K. H., & Tardieu, M. (1995). Establishment of human microglial cell lines after transfection of primary cultures of embryonic microglial cells with the SV40 large T antigen. *Neuroscience Letters, 195*(2), 105–108. Retrieved from https://www.ncbi.nlm.nih.gov/pubmed/7478261

Kataoka, N., Bachorik, J. L., & Dreyfuss, G. (1999). Transportin-SR, a nuclear import receptor for SR proteins. *The Journal of Cell Biology*, *145*(6), 1145–1152. Retrieved from https://www.ncbi.nlm.nih.gov/pubmed/10366588

Lambotte, O., Deiva, K., & Tardieu, M. (2006). HIV-1 Persistence, Viral Reservoir, and the Central Nervous System in the HAART Era. *Brain Pathology*, *13*(1), 95–103. https://doi.org/10.1111/j.1750-3639.2003.tb00010.x

Lee, K., Ambrose, Z., Martin, T. D., Oztop, I., Mulky, A., Julias, J. G., … KewalRamani, V. N. (2010). Flexible use of nuclear import pathways by HIV-1. *Cell Host & Microbe*, *7*(3), 221–233. https://doi.org/10.1016/j.chom.2010.02.007

Li, Y.-L., Chandrasekaran, V., Carter, S. D., Woodward, C. L., Christensen, D. E., Dryden, K. A., … Sundquist, W. I. (2016). Primate TRIM5 proteins form hexagonal nets on HIV-1 capsids. *eLife*, *5*. https://doi.org/10.7554/eLife.16269

Lukic, Z., Dharan, A., Fricke, T., Diaz-Griffero, F., & Campbell, E. M. (2014). HIV-1 uncoating is facilitated by dynein and kinesin 1. *Journal of Virology*, *88*(23), 13613–13625. https://doi.org/10.1128/JVI.02219-14

Mamede, J. I., Sitbon, M., Battini, J.-L., & Courgnaud, V. (2013). Heterogeneous susceptibility of circulating SIV isolate capsids to HIV-interacting factors. *Retrovirology*, *10*, 77. https://doi.org/10.1186/1742-4690-10-77

McDonald, D., Vodicka, M. A., Lucero, G., Svitkina, T. M., Borisy, G. G., Emerman, M., & Hope, T. J. (2002). Visualization of the intracellular behavior of HIV in living cells. *The Journal of Cell Biology*, *159*(3), 441–452. https://doi.org/10.1083/jcb.200203150

National Institute of Health. (2019). Guidelines for the Use of Antiretroviral Agents in Adults and Adolescents Living with HIV. Retrieved from https://aidsinfo.nih.gov/contentfiles/lvguidelines/AA_Tables.pdf

Nepveu-Traversy, M.-E., Bérubé, J., & Berthoux, L. (2009). TRIM5alpha and TRIMCyp form apparent hexamers and their multimeric state is not affected by exposure to restriction-sensitive viruses or by treatment with pharmacological inhibitors. *Retrovirology*, *6*, 100. https://doi.org/10.1186/1742-4690-6-100

Nimmerjahn, A., Kirchhoff, F., & Helmchen, F. (2005). Resting microglial cells are highly dynamic surveillants of brain parenchyma in vivo. *E-Neuroforum*, *11*(3). https://doi.org/10.1515/nf-2005-0304

Nisole, S., Lynch, C., Stoye, J. P., & Yap, M. W. (2004). A Trim5-cyclophilin A fusion protein found in owl monkey kidney cells can restrict HIV-1. *Proceedings of the National Academy of Sciences of the United States of America*, *101*(36), 13324–13328. https://doi.org/10.1073/pnas.0404640101

Peng, K., Muranyi, W., Glass, B., Laketa, V., Yant, S. R., Tsai, L., … Kräusslich, H.-G. (2014). Quantitative microscopy of functional HIV post-entry complexes reveals association of replication with the viral capsid. *eLife*, *3*, e04114. https://doi.org/10.7554/eLife.04114

Pornillos, O., Ganser-Pornillos, B. K., & Yeager, M. (2011). Atomic-level modelling of the HIV capsid. *Nature*, *469*(7330), 424–427. https://doi.org/10.1038/nature09640

Price, A. J., Fletcher, A. J., Schaller, T., Elliott, T., Lee, K., KewalRamani, V. N., … James, L. C. (2012). CPSF6 defines a conserved capsid interface that modulates HIV-1 replication. *PLoS Pathogens*, *8*(8), e1002896. https://doi.org/10.1371/journal.ppat.1002896

Qi, M., Yang, R., & Aiken, C. (2008). Cyclophilin A-dependent restriction of human immunodeficiency virus type 1 capsid mutants for infection of nondividing cells. *Journal of Virology*, *82*(24), 12001–12008. https://doi.org/10.1128/JVI.01518-08

Saijo, K., & Glass, C. K. (2011). Microglial cell origin and phenotypes in health and disease. *Nature Reviews. Immunology*, *11*(11), 775–787. https://doi.org/10.1038/nri3086

Schaller, T., Ocwieja, K. E., Rasaiyaah, J., Price, A. J., Brady, T. L., Roth, S. L., … Towers, G. J. (2011). HIV-1 capsid-cyclophilin interactions determine nuclear import pathway, integration targeting and replication efficiency. *PLoS Pathogens*, *7*(12), e1002439. https://doi.org/10.1371/journal.ppat.1002439

Shah, V. B., Shi, J., Hout, D. R., Oztop, I., Krishnan, L., Ahn, J., … Aiken, C. (2013). The host proteins transportin SR2/TNPO3 and cyclophilin A exert opposing effects on HIV-1 uncoating. *Journal of Virology*, *87*(1), 422–432. https://doi.org/10.1128/JVI.07177-11

Strambio-De-Castillia, C., Niepel, M., & Rout, M. P. (2010). The nuclear pore complex: bridging nuclear transport and gene regulation. *Nature Reviews. Molecular Cell Biology*, *11*(7), 490–501. https://doi.org/10.1038/nrm2928

von Schwedler, U. K., Stray, K. M., Garrus, J. E., & Sundquist, W. I. (2003). Functional surfaces of the human immunodeficiency virus type 1 capsid protein. *Journal of Virology*, *77*(9), 5439–5450. Retrieved from https://www.ncbi.nlm.nih.gov/pubmed/12692245

UNAIDS. (2018). Fact sheet - Latest statistics on the status of the AIDS epidemic. Retrieved from http://www.unaids.org/en/resources/fact-sheet

Withers-Ward, E. S., Kitamura, Y., Barnes, J. P., & Coffin, J. M. (1994). Distribution of targets for avian retrovirus DNA integration in vivo. *Genes & Development*, *8*(12), 1473–1487. https://doi.org/10.1101/gad.8.12.1473

Yamashita, M., Perez, O., Hope, T. J., & Emerman, M. (2007). Evidence for direct involvement of the capsid protein in HIV infection of nondividing cells. *PLoS Pathogens*, *3*(10), 1502–1510. https://doi.org/10.1371/journal.ppat.0030156

Yang, Y., Luban, J., & Diaz-Griffero, F. (2014). The fate of HIV-1 capsid: a biochemical assay for HIV-1 uncoating. *Methods in Molecular Biology*, *1087*, 29–36. https://doi.org/10.1007/978-1-62703-670-2_3

Zhang, R., Mehla, R., & Chauhan, A. (2010). Perturbation of Host Nuclear Membrane Component RanBP2 Impairs the Nuclear Import of Human Immunodeficiency Virus -1 Preintegration Complex (DNA). *PLoS ONE*, *5*(12). https://doi.org/10.1371/journal.pone.0015620

Zhou, L., Sokolskaja, E., Jolly, C., James, W., Cowley, S. A., & Fassati, A. (2011). Transportin 3 promotes a nuclear maturation step required for efficient HIV-1 integration. *PLoS Pathogens*, *7*(8), e1002194. https://doi.org/10.1371/journal.ppat.1002194